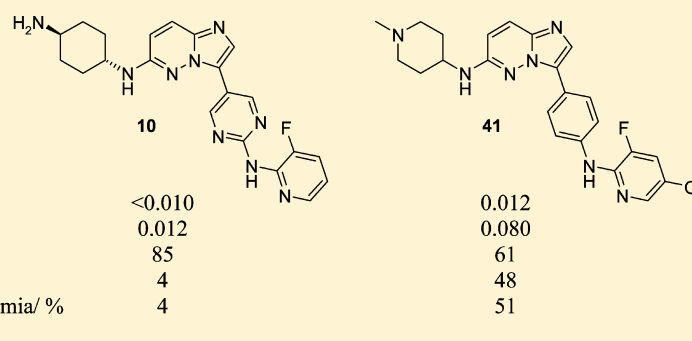


Optimization of an Imidazopyridazine Series of Inhibitors of *Plasmodium falciparum* Calcium-Dependent Protein Kinase 1 (PfCDPK1)

Timothy M. Chapman,^{*,†} Simon A. Osborne,[†] Claire Wallace,[†] Kristian Birchall,[†] Nathalie Bouloc,[†] Hayley M. Jones,[†] Keith H. Ansell,[†] Debra L. Taylor,[†] Barbara Clough,[‡] Judith L. Green,[‡] and Anthony A. Holder[‡]

[†]Centre for Therapeutics Discovery, MRC Technology, 1-3 Burtonhole Lane, Mill Hill, London NW7 1AD, U.K.

[‡]Division of Parasitology, MRC National Institute for Medical Research, The Ridgeway, Mill Hill, London NW7 1AA, U.K.



ABSTRACT: A structure-guided design approach using a homology model of *Plasmodium falciparum* calcium-dependent protein kinase 1 (*Pf*CDPK1) was used to improve the potency of a series of imidazopyridazine inhibitors as potential antimalarial agents. This resulted in high affinity compounds with *Pf*CDPK1 enzyme IC₅₀ values less than 10 nM and *in vitro* *P. falciparum* antiparasite EC₅₀ values down to 12 nM, although these compounds did not have suitable ADME properties to show *in vivo* efficacy in a mouse model. Structural modifications designed to address the ADME issues, in particular permeability, were initially accompanied by losses in antiparasite potency, but further optimization allowed a good balance in the compound profile to be achieved. Upon testing *in vivo* in a murine model of efficacy against malaria, high levels of compound exposure relative to their *in vitro* activities were achieved, and the modest efficacy that resulted raises questions about the level of effect that is achievable through the targeting of *Pf*CDPK1.

INTRODUCTION

Malaria is one of the most prevalent infectious diseases of the developing world. In excess of 3 billion people are at risk, and it currently leads to the deaths of around 655,000 people each year, with the majority of these occurring in sub-Saharan Africa among children under five years of age.¹ Resistance to existing antimalarial drugs is widespread,² and therefore, new therapeutic approaches are urgently needed. Calcium-dependent protein kinases (CDPKs) are directly regulated by Ca²⁺ and are found in plants and organisms in the alveolate lineage,³ but they are absent in humans. They are present in *Apicomplexan* parasites including *Plasmodium falciparum*, the causative agent of the most severe form of malaria. CDPKs in *Plasmodium* are present as a multigene family containing at least five members,⁴ and different CDPKs are proposed to be functional at different stages of the parasite life cycle. *P. falciparum* calcium-dependent protein kinase 1 (*Pf*CDPK1), first identified by Zhao et al.,⁵ is expressed in the asexual blood stages of the parasite responsible for disease pathology. It has been shown to be encoded by an important gene,^{6,7} and it is implicated in parasite motility and

host cell invasion, where it is able to phosphorylate components of the molecular motor that drives parasite invasion of red blood cells.^{8,9} The prevention of this invasion process could break the parasite lifecycle, causing the parasites to die and the infection to be cleared. *Pf*CDPK1 therefore represents a novel target for the potential treatment of malaria and offers promise for achieving selectivity over the kinases of the human host. More recently, its role in translational regulation of motor complex transcripts in gametocytes¹⁰ and in schizont development¹¹ has also been reported. There has been interest in CDPKs as drug targets,¹² although relatively few inhibitors have been reported in the literature: Kato et al.⁷ and Lemerrier et al.¹³ have reported inhibitors of *Pf*CDPK1, and inhibitors of the CDPK1 enzymes from the related *Apicomplexan* protozoa *Toxoplasma gondii* and *Cryptosporidium parvum* have also been described.^{14–16}

Received: March 4, 2014

Published: April 1, 2014

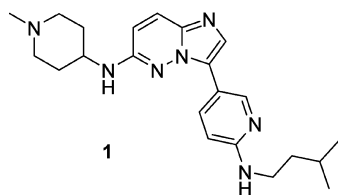


Figure 1. Summary data for compound 1.

A high throughput screen of our compound collection against the isolated recombinant *Pf*CDPK1 enzyme identified a hit series containing an imidazopyridazine core as the primary series of interest, and the initial development of the structure–activity relationship (SAR) in this series has been described previously.¹⁷ Compounds with potent enzyme inhibitory activity had been generated, which also showed good kinase selectivity against a human kinase panel and promising *in vitro* ADME profiles. In particular, compound 1 (Figure 1) represented an early lead, with low nanomolar inhibitory potency against *Pf*CDPK1, sub-500 nM antiparasite activity, and modest *in vivo* efficacy in a *P. berghei* mouse model of malaria.

In order to advance this series, improvements were sought in the *in vitro* antiparasite activity and pharmacokinetic profile of the series while maintaining a good selectivity profile against human kinases to generate compounds with the potential to show improved *in vivo* efficacy.

RESULTS AND DISCUSSION

A structure-guided design approach using a homology model of *Pf*CDPK1 (based on *Tg*CDPK1, PDB ref: 3I7C)¹⁸ was used in attempting to gain increased binding affinity against the target and correspondingly increase the cellular potency of the inhibitors. The homology model had proved effective in explaining the SAR up to this point, and it was therefore used as a key component in considering how additional potency could be gained. In particular, it suggested that the binding pocket occupied by the isopentyl chain of compound 1 was not optimally filled and that there was potential to gain additional beneficial interactions with the enzyme in this region. Virtual libraries were enumerated with a diverse range of groups at this position and examined through docking using Glide SP.¹⁹ For enumeration purposes, the basic amine group was set to be either *N*-methylpiperidine or 1,4-diaminocyclohexane, which had been previously demonstrated to be optimal for potency,¹⁷ and the heteroaryl linker ring was set as either pyridine or pyrimidine. Analysis of the docking results suggested that replacement of the isopentyl group with an aromatic ring containing a suitably positioned hydrogen-bond acceptor (for example, a 2-pyridyl group, as in compound 2; Figure 2) could give increased binding affinity.

In comparison with the isopentyl group in this pocket, the 2-pyridyl nitrogen atom could potentially form an additional hydrogen-bond interaction with the backbone N-H of Asp-212 (depicted in Figure 3B), and it also appeared to be an excellent spatial and electrostatic fit into the rest of this pocket. Compound 2 was predicted to be able to retain the other key interactions made by compound 1: a hydrogen bond between the imidazopyridazine core and the backbone N-H of

*Pf*CDPK1 IC₅₀ = 0.013 μM
P. falciparum EC₅₀ = 0.40 μM
 m log D = 3.4
 MLM % rem at 30 min = 63
 HLM % rem at 40 min = 85
 PAMPA P_{app} = 81 nm/s
 Mouse iv t_{1/2} = 2.0 h
 Mouse ppb = 86%
In vivo reduction in parasitaemia = 46%
 (*P. berghei*, 50 mg/kg, po qd, 4 days)

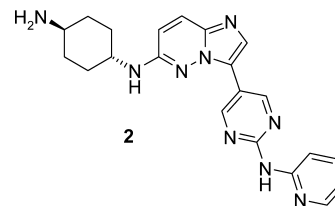


Figure 2. Example of the 2-pyridyl variant with superior predicted binding affinity from docking studies.

Tyr-148 at the hinge region, a hydrogen bond with the side-chain carboxylic acid of Asp-212, and an additional hydrogen bond between the basic amine group and Glu-152 as it points out toward the solvent.

The top scoring compounds identified from the docking studies were then synthesized according to the route in Scheme 1. Intermediate 3 was functionalized through nucleophilic substitution on the chloro- at the 6-position to install the BOC-protected amine side chains in intermediates 4 and 17. These were elaborated through Suzuki coupling with the appropriate boronate reagents to give the 5-aminopyrimidine products 5 and 18, the 5-thiomethylpyrimidine 13 or 5-aminopyridine 20. The final compounds were prepared by either a Buchwald coupling with an aryl halide or through oxidation of the thiomethyl pyrimidine followed by nucleophilic displacement with the appropriate amine.

The SAR of the synthesized analogues is shown in Table 1. As predicted by the docking studies, variants containing a 2-pyridyl or phenyl group at this position both showed increased binding affinity to the enzyme versus compound 1 (Table 1, examples 2 and 6). As the potency of the most potent compounds was now below the limit of detection of our primary Kinase Glo enzyme assay, a thermal denaturation assay was used to quantify the differences and define a rank order in binding affinity between the most potent compounds.²⁰ This revealed that the 2-pyridyl compound 2 resulted in a larger shift in the thermal denaturation temperature of the protein (ΔT_m) than its phenyl counterpart 6, and both showed a higher thermal shift than compound 1 in this assay, which displayed a ΔT_m of 15.7 K. Gratifyingly, this difference in enzyme affinity was reflected in the potency of the compounds against the *P. falciparum* parasite, with compound 2 showing an EC₅₀ of 80 nM compared with 180 nM for compound 6.

Alternative heteroaryl groups were then explored: 2-pyrazine 7 showed good potency, albeit weaker than those of 2 and 6, but 3-pyridyl 8 and 2-pyrimidyl 9 lost potency against both the enzyme and parasite. The addition of substituents to the pyridyl ring was investigated: 3-fluoropyridyl gave a boost in potency against both the enzyme and the parasite, with compound 10 displaying a high thermal shift of 28.0 K and excellent EC₅₀ of

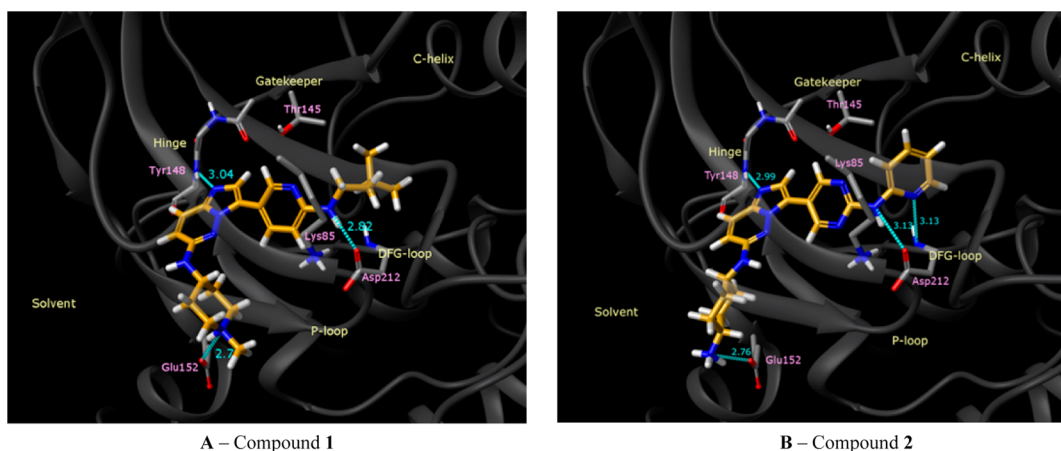
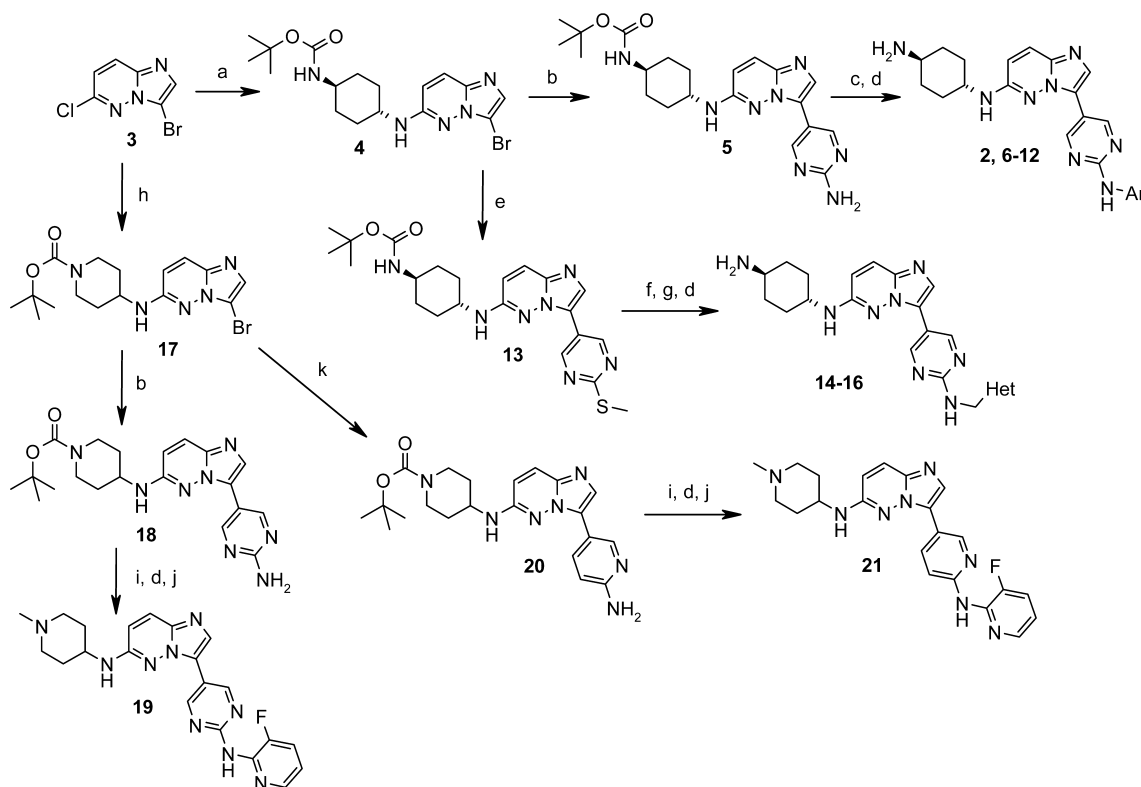


Figure 3. Proposed binding modes from the docking of compound 1 (A) and compound 2 (B) illustrating the potential to gain an additional H-bond interaction with the backbone N-H of Asp-212.

Scheme 1. Synthetic Route to Heteroaryl and Aryl Variants^a

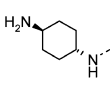
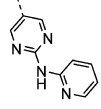
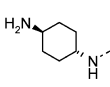
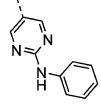
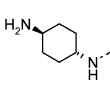
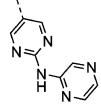
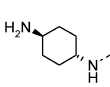
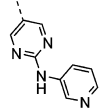
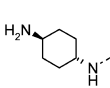
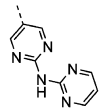
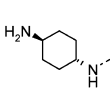
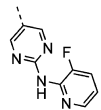
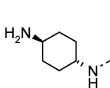
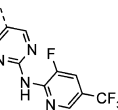
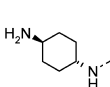
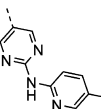
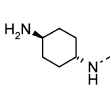
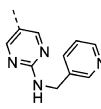
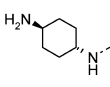
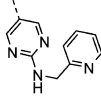
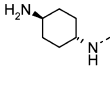
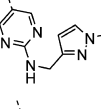
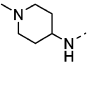
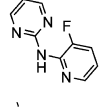
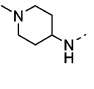
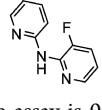


^aReagents and conditions: (a) *trans*-cyclohexane-1,4-diamine, NMP, microwave, 180 °C, then di-*tert*-butyl dicarbonate, DMAP, Et₃N, THF, reflux; (b) 2-aminopyrimidine-5-boronic acid pinacol ester, Pd(dppf)Cl₂, Cs₂CO₃, dioxane/water, 90 °C; (c) aryl/heteroaryl halide, Pd(OAc)₂, CyPF-Bu or Xantphos, NaO^tBu or Cs₂CO₃, DME or dioxane, 80 °C; (d) 4 M HCl/dioxane, MeOH; (e) 2-(thiomethyl)pyrimidine-5-boronic acid, Pd(dppf)Cl₂, Cs₂CO₃, dioxane/water, 90 °C; (f) *m*-chloroperoxybenzoic acid, CH₂Cl₂; (g) 3-(aminomethyl)pyridine or 2-(aminomethyl)pyridine or (1-methyl-1*H*-pyrazol-3-yl)methylamine, dioxane, reflux; (h) *tert*-butyl 4-aminopiperidine-1-carboxylate, DIPEA, NMP, 130 °C; (i) 2-chloro-3-fluoropyridine, Pd(OAc)₂, Xantphos, Cs₂CO₃, dioxane, microwave, 130 °C or thermal, 90 °C; (j) formaldehyde, AcOH, sodium triacetoxyborohydride, THF; (k) 2-aminopyridine-5-boronic acid pinacol ester, Pd(dppf)Cl₂, Cs₂CO₃, dioxane/water, 90 °C.

12 nM against the parasite. The introduction of 5-position substituents to the pyridine ring such as trifluoromethyl (**11**) and methyl (**12**) led to excellent enzyme affinity and increased thermal shift values relative to **10**, although their antiparasite potency decreased. When a CH₂ spacer group was introduced, the 3-pyridyl variant **14** was relatively weak against the enzyme, whereas the 2-pyridyl variant **15** and the 3-pyrazole **16** showed good enzyme inhibitory potency. This was again consistent

with the predictions of the homology model, which suggested that **15** could form an H-bond with Asp-212, whereas **14** could not. However, all of these variants were weak against the parasite. Switching to the *N*-methylpiperidine basic side chain (**19**) gave good potency against the enzyme and the parasite, while changing the pyrimidine linker ring to a pyridyl linker ring (**21**) retained high enzyme potency but led to a loss in potency against the parasite.

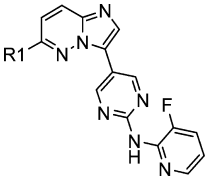
Table 1. *In Vitro* Potency Data for Aryl and Heteroaryl Variants

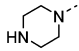
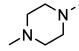
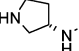
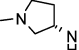
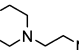
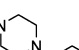
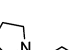
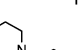
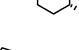
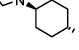
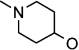
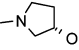
Compound	R1	R2	<i>Pf</i> CDPK1 IC ₅₀ ^a μM	Thermal shift ΔT _m / K	<i>P. falciparum</i> EC ₅₀ ^a μM
2			<0.010	22.4	0.08
6			<0.010	18.9	0.18
7			0.014	20.4	0.31
8			0.066	<i>nt</i>	0.66
9			0.061	<i>nt</i>	2.0
10			<0.010	28.0	0.012
11			<0.010	30.4	0.27
12			<0.010	32.0	0.46
14			0.049	<i>nt</i>	0.73
15			0.014	17.9	1.5
16			0.019	<i>nt</i>	3.2
19			0.013	25.4	0.07
21			<0.010	23.6	0.39

^aThe limit of detection of the *Pf*CDPK1 Kinase Glo enzyme assay is 0.010 μM; *nt* = not tested.

Leading compounds were profiled in *in vitro* ADME assays, and selected data are shown in Table 2. In general, the

compounds had low measured log *D* values and displayed good stability in both mouse and human microsomes but poor

Table 3. *In Vitro* Potency, Properties, and Permeability Data for Selected Variations on the Basic Amine Side Chain


Compound	R1	<i>Pf</i> CDPK1 IC ₅₀ / μM	ΔT _m / K	<i>P. falciparum</i> EC ₅₀ / μM	Calc. pK _a ^a	m log D	PAMPA P _{app} /nms ⁻¹
22	H ₃ C ⁺	0.044	<i>nt</i>	>1	3.0	2.5	138
23		0.021	<i>nt</i>	0.27	8.4	0.7	4
24		0.022	<i>nt</i>	0.80	7.1	2.2	61
25		<0.010	21.0	0.11	9.6	0.4	0
26		<0.010	20.0	0.26	9.4	1.5	2
27		0.040	<i>nt</i>	>1	6.7	2.9	27
28		0.036	<i>nt</i>	0.22	7.6	1.6	4
29		0.045	16.0	>1	9.8	1.5	6
30		0.011	22.5	0.034	7.8	3.2	17
31		<0.010	22.5	0.036	10.4	1.9	3
32		<0.010	20.5	>1	7.7	1.5	27
33		0.019	15.5	>1	8.3	1.5	28
34		0.014	22.1	0.77	9.1	1.3	4

^apK_a of conjugate acid calculated according to ref 22; *nt* = not tested.

improved antiparasite activity relative to the *N*-methylpiperidines. Reverting to the diaminocyclohexane basic group with a free -NH₂ (**40**) gave improved antiparasite activity but reduced permeability, and variants with a pyrazole linker ring were also investigated, and these have been described previously.²³

In summary, although modifications of this linker ring led to significant and steep improvements in PAMPA permeability, the variations that gave improved permeability versus compound **10** while maintaining good enzyme inhibitory potency were also accompanied by a significant loss in antiparasite activity. Although the desired balance in compound profile had not yet been achieved through modification of this group, the higher permeability of these compounds warranted pharmacokinetic studies to confirm that they could achieve good *in vivo* exposure.

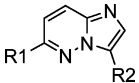
Pharmacokinetics. Pharmacokinetic profiling in rats revealed that there was a good correlation between *in vitro*

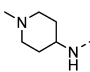
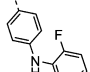
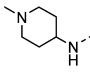
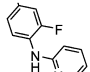
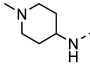
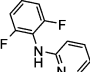
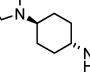
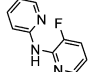
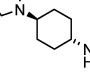
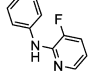
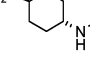
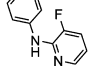
ADME and *in vivo* PK, with compound **35** showing the best PK profile of those tested (data shown in Table 5).

Compounds **35**, **38**, and **39** were then advanced to testing in the *P. berghei* *in vivo* mouse model, and despite their lower antiparasite potency compared to that of earlier examples such as compound **10**, they showed superior efficacy. The observed efficacy was still only modest, with best results of 44% and 46% reduction in parasitemia achieved with **35** and **38**, respectively, at a 50 mg/kg oral dose (Table 6).

In order to evaluate the exposure in the efficacy model, blood samples were taken for compound **35**, which revealed that it had achieved a good exposure with total plasma levels of 1660 ng/mL at 1 h (10-fold over the antiparasite EC₅₀) and 1460 ng/mL at 4 h (8.5-fold over the antiparasite EC₅₀).

Addressing Species Differences between *P. falciparum* and *P. berghei*. As the *in vivo* efficacy model is performed with the rodent parasite *P. berghei* rather than *P. falciparum*, there remained a possibility that the low *in vivo* efficacy

Table 4. *In Vitro* Potency and Permeability Data for R2 Linker Ring Variations^a


Compound	R1	R2	<i>Pf</i> CDPK1 IC ₅₀ / μM	ΔT _m / K	<i>P. falciparum</i> EC ₅₀ / μM	PAMPA P _{app} /nms ⁻¹
35			0.016	21.1	0.41	171
36			0.011	22.1	0.40	101
37			0.026	<i>nt</i>	0.48	103
38			0.019	22.2	0.30	92
39			0.016	19.7	0.29	81
40			0.034	<i>nt</i>	0.14	15

^a*nt* = not tested.Table 5. Pharmacokinetics of Compound 35 in Rats^a

iv <i>t</i> _{1/2} (h)	4
plasma Cl (mL/min/kg)	28
blood Cl (mL/min/kg)	14
<i>V</i> _d (L/kg)	8
oral BA (%)	70

^aCompound dosed as hydrochloride salt, iv in aqueous vehicle containing 0.9% (w/v) NaCl at 4.5 mg/kg; po in aqueous vehicle containing 0.5% (w/v) hydroxypropylmethylcellulose, 0.5% (v/v) benzyl alcohol, and 0.4% (v/v) Tween-80 at 21 mg/kg.

Table 6. *In Vitro* ADME and *In Vivo* Efficacy Data for Selected Compounds

compd	HLM (% rem) ^a	MLM (% rem) ^b	<i>m log D</i>	PAMPA P _{app} /nms ⁻¹	<i>in vivo</i> reduction in parasitemia ^c
35	80	47	3.2	171	44
38	71	88	2.8	92	46
39	60	82	3.3	81	34

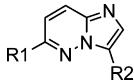
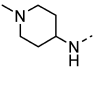
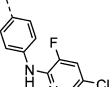
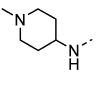
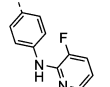
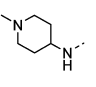
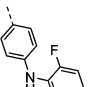
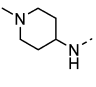
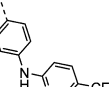
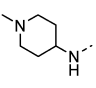
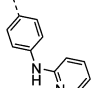
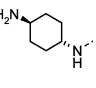
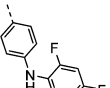
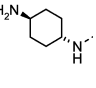
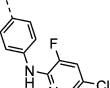
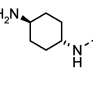
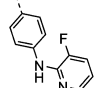
^aPercent remaining at 40 min. ^bPercent remaining at 30 min. ^cMeasured in the *P. berghei* mouse model of malaria, 4-day Peters test with oral dosing once daily at 50 mg/kg; compounds were dosed as monohydrochloride salts, dissolved in 30:70 EtOH/Tween-80, and diluted 10-fold with water prior to dosing.

achieved might be due to species differences. Significant efficacy differences across the parasite species have been observed in the development of other antimalarial compounds, and therefore, it was desirable to address this possibility. First, an *in silico* assessment of *Pf*CDPK1 and *Pb*CDPK1 revealed that across their entire protein sequences *Pb*CDPK1 and *Pf*CDPK1 have high homology, with 88% sequence identity and 93% similarity.

Furthermore, based on the residues within 10 Å of any atom of ATP in the *Pb*CDPK1 crystal structure (PDB ID: 3Q51), there is 100% identity. Docking of the inhibitors into the ATP-binding site of *Pb*CDPK1 predicted that they would bind with an affinity similar to that for *Pf*CDPK1. This prediction was confirmed through the expression of the recombinant *Pb*CDPK1 enzyme and measurement of the IC₅₀ values, which showed that key compounds bound with similar affinity between the two enzymes (representative compounds 1 and 35 showed *Pb*CDPK1 IC₅₀ values of 22 and 15 nM, respectively). Finally, in order to probe *in vivo* differences, selected compounds were tested in a *P. falciparum* murine model, in which a severe combined immunodeficient (SCID) mouse can be injected with human erythrocytes infected with a suitable strain of *P. falciparum* parasites.²⁴ Compounds 1 and 35 were tested in this efficacy model with the same dosing regimen as in the *P. berghei* model (50 mg/kg, oral, once daily), but disappointingly, no efficacy was observed despite good compound exposure.

In parallel with *in vivo* testing, efforts had also been focused on achieving an improved compound profile with respect to the combination of antiparasite potency and pharmacokinetics. Although modification of the linker ring had led to improved pharmacokinetics, this had been achieved at the expense of antiparasite potency, so attention then turned to the distal pyridyl ring as a point of modification to potentially restore potency. The introduction of substituents around this ring had previously produced compounds with the highest enzyme affinities as determined by thermal denaturation experiments (Table 1, compounds 11 and 12), so this approach offered the potential to yield increased antiparasite potency. Molecular

Table 7. *In Vitro* Potency and ADME Data for Distal Pyridyl Ring Substitution Variants

Compound	R1	R2			HLM (% rem) ^a	MLM (% rem) ^b	m log D	PAMPA P _{app} / nms ⁻¹
			<i>Pf</i> CDPK1 IC ₅₀ / μM	<i>P. falciparum</i> EC ₅₀ / μM				
41			0.012	0.08	86	61	3.7	48
42			0.019	0.10	77	52	3.5	76
43			0.015	0.20	78	58	3.7	77
44			0.014	0.05	81	85	3.7	51
45			0.029	0.03	80	73	3.4	63
46			0.017	0.12	68	87	2.0	26
47			<0.010	0.30	77	57	3.1	64
48			0.014	0.08	83	90	2.2	54

^aPercent remaining at 40 min. ^bPercent remaining at 30 min.

modeling suggested that there was sufficient space in the binding pocket for small substituents to be accommodated, so a number of variants were synthesized, and the resulting SAR is shown in Table 7. With *N*-methylpiperidine as the basic group and a phenyl linker ring in place, the addition of 5-chloro (**41**), 6-methyl (**42**), or 5-fluoro (**43**) substituents was well tolerated, with sub-100 nM antiparasite EC₅₀ values for **41** and **42** and acceptable *in vitro* ADME. The 5- and 6-trifluoromethyl substituted pyridines **44** and **45** also showed excellent antiparasite EC₅₀ values of 50 and 30 nM, respectively, with good *in vitro* ADME characteristics. Compounds **46–48**, with the diaminocyclohexane basic group, also showed a good balance between antiparasite activity and ADME properties; in particular, compound **48** demonstrated the best profile with an antiparasite EC₅₀ of 80 nM combined with high stability in mouse and human microsomes and acceptable permeability.

Compounds **41** and **48** were advanced to the *P. berghei* *in vivo* mouse model; however, they did not show significantly improved efficacy compared to that of previous examples (Table 8), and a maximum of 51% reduction in parasitemia was achieved with compound **41**. Blood samples revealed that

Table 8. *In Vivo* Efficacy Data and Total Plasma Levels of Compounds **41** and **48** in the *P. berghei* Mouse Model^a

compd	41	48
<i>in vivo</i> reduction in parasitemia ^a	51	18
plasma concentration at 4 h/ng mL ⁻¹ (fold exposure over <i>in vitro</i> EC ₅₀)	1610 (45×)	621 (18×)
plasma concentration at 24 h/ng mL ⁻¹ (fold exposure over <i>in vitro</i> EC ₅₀)	1270 (35×)	6.54 (0.2×)

^aFour-day Peters test with once daily oral dosing at 50 mg/kg; compounds were dosed as monohydrochloride salts, dissolved in 30:70 EtOH/Tween-80, and diluted 10-fold with water prior to dosing.

compound **41** had achieved a good exposure (total plasma concentration 45-fold over *in vitro* antiparasite EC₅₀ at 4 h and 35-fold at 24 h), whereas **48** showed lower exposure, consistent with its lower observed *in vivo* efficacy.

CONCLUSIONS

An imidazopyridazine series of *Pf*CDPK1 inhibitors was optimized employing a structure-guided design approach with

a homology model of PfCDPK1. Initial 2-pyridyl variants showed excellent potency in assays against the PfCDPK1 enzyme and *P. falciparum* parasite but did not possess sufficient permeability to be effective *in vivo*. Modifications of the basic side chain and aryl linker rings allowed permeability to be improved, but this led to a reduction in antiparasite potency. Finally, further optimization of the linker ring and distal pyridyl ring led to molecules possessing well-balanced profiles with respect to potency and *in vitro* ADME and suitable for *in vivo* dosing, with high resulting compound exposures following oral administration.

However, despite the improvements made to the compound profiles compared with those of the early lead compound **1**, the *in vivo* reduction in parasitemia in a murine *P. berghei* model of malaria remained modest, with a maximum reduction of 51% with an oral dose of 50 mg/kg for compound **41**. The reason for this limited effect remains unclear: although the PfCDPK1 enzyme has been shown to be encoded by an important gene in the malaria parasite and high levels of *in vivo* compound exposure were achieved relative to *in vitro* antiparasite EC₅₀, it may be that a higher multiple of this EC₅₀ is required for a longer period of time to produce higher efficacy or that low levels of residual CDPK1 enzyme activity may be sufficient for parasite survival. There may be a level of redundancy allowing a CDPK1-based inhibitory effect to be circumvented, and indeed, a recent report has suggested that CDPK1 may not in fact be required for host cell invasion in the erythrocytic stage in *Plasmodium berghei* but rather that it plays an essential role in the mosquito sexual stages.²⁵ Differences in parasite biology may also explain the limited effect of the inhibitors *in vivo*: for example, *P. berghei* has only a 24-h multiplication cycle and develops in reticulocytes in the mouse compared with a 48-h cycle in mature red cells for *P. falciparum*, and differences in synchrony of parasite development may also have contributed to the reduced efficacy of the compounds. Further studies on these compounds including understanding their mechanism of action, the identification of additional CDPK1 substrates, and the development of better read-outs of activity are ongoing, and these will be reported in future publications.

EXPERIMENTAL SECTION

Chemistry. All commercial reagents and solvents were used without further purification. Silica gel chromatography was carried out using a Biotage SP4 or Isolera MPLC system with prepacked silica gel cartridges. Preparative HPLC was carried out using an apparatus made by Agilent. The apparatus is constructed such that the chromatography (column: either a 19 × 100 mm (5 μm) C-18 Waters Xbridge or a 19 × 100 mm (5 μm) C-6Ph Waters Xbridge column, both at a flow rate of 40 mL/min) is monitored by a multiwavelength UV detector (G1365B manufactured by Agilent) and an MM-ES + APCI mass spectrometer (G-1956A, manufactured by Agilent) connected in series, and if the appropriate criteria are met, the sample is collected by an automated fraction collector (G1364B manufactured by Agilent). Collection was triggered by a combination of UV or mass spectrometry or based on time. Typical conditions for the separation process are as follows: the gradient was run over a 7 min period (gradient at the start, 10% methanol and 90% water; and gradient at the finish, 100% methanol and 0% water; as buffer, 0.1% formic acid, 0.1% ammonium hydroxide, or 0.1% trifluoroacetic acid was added to the water). Purity of all final derivatives for biological testing was confirmed to be >95% as determined using the following conditions: an Agilent HPLC instrument with a C-18 Xbridge column (3.5 μm, 4.6 × 30 mm, gradient at the start, 10% acetonitrile and 90% water; gradient at the finish, 100% acetonitrile and 0% water; as buffer, either 0.1% ammonium hydroxide or 0.1% trifluoroacetic acid was added to

the water). A flow rate of 3 mL/min was used with UV detection at 254 and 210 nm. The structure of the intermediates and final products was confirmed by ¹H NMR spectroscopy and mass spectrometry. ¹H nuclear magnetic resonance (NMR) spectroscopy was carried out using a JEOL ECX400 spectrometer in the stated solvent at around room temperature unless otherwise stated. Characteristic chemical shifts (δ) are given in parts-per-million using conventional abbreviations for the designation of major peaks: e.g., s, singlet; d, doublet; t, triplet; q, quartet; dd, doublet of doublets; and br, broad. Analytical mass spectra were recorded using a MM-ES + APCI or ES mass spectrometer (G-1956A or G-6120B, manufactured by Agilent).

tert-Butyl {trans-4-[[3-bromoimidazo[1,2-b]pyridazin-6-yl]amino]cyclohexyl}carbamate 4. (a) A solution of 3-bromo-6-chloroimidazo[1,2-b]pyridazine **3** (1.40 g, 6.02 mmol) in NMP (8 mL) was treated with *trans*-cyclohexane-1,4-diamine (2.05 g, 18.0 mmol, 3.0 equiv) and stirred with microwave heating at 180 °C for 30 min. It was then diluted with EtOAc (100 mL) and washed with water (2 × 100 mL). The organic layer was dried and concentrated under reduced pressure. Chromatography on silica gel (2 M NH₃ in MeOH/EtOAc gradient) gave *trans*-N-(3-bromo-imidazo[1,2-b]pyridazin-6-yl)-cyclohexane-1,4-diamine as a pale yellow solid (981 mg, 52%). ¹H NMR (400 MHz, DMSO-*d*₆) δ ppm 7.66 (d, *J* = 10.1 Hz, 1H), 7.45 (s, 1H), 6.95 (br. d, *J* = 7.3 Hz, 1H), 6.65 (d, *J* = 9.6 Hz, 1H), 3.63–3.53 (m, 1H), 2.60–2.52 (m, 1H), 2.08–2.04 (m, 2H), 1.82–1.78 (m, 2H), 1.28–1.09 (m, 4H). *m/z* (ES + APCI)⁺: 310/312 [M + H]⁺. (b) A solution of *trans*-N-(3-bromo-imidazo[1,2-b]pyridazin-6-yl)-cyclohexane-1,4-diamine (1.80 g, 5.79 mmol) in THF (20 mL) was treated with Et₃N (1.21 mL, 8.70 mmol, 1.5 equiv), di-*tert*-butyl dicarbonate (1.90 g, 8.70 mmol, 1.5 equiv), and DMAP (71 mg, 0.58 mmol, 0.1 equiv) and stirred at reflux for 18 h. Concentration under reduced pressure and silica gel chromatography (20% MeOH/EtOAc) gave **4** as a pale yellow solid (1.60 g, 67%). ¹H NMR (400 MHz, DMSO-*d*₆) δ ppm 7.67 (d, *J* = 9.6 Hz, 1H), 7.46 (s, 1H), 6.99 (br. d, *J* = 7.3 Hz, 1H), 6.76 (br. d, *J* = 8.2 Hz, 1H), 6.65 (d, *J* = 9.6 Hz, 1H), 3.59–3.52 (m, 1H), 3.28–3.22 (m, 1H), 2.11–2.08 (m, 2H), 1.84–1.81 (m, 2H), 1.38 (s, 9H), 1.30–1.23 (m, 4H). *m/z* (ES + APCI)⁺: 410/412 [M + H]⁺.

tert-Butyl (trans-4-[[3-(2-aminopyrimidin-5-yl)imidazo[1,2-b]pyridazin-6-yl]amino]cyclohexyl)carbamate 5. A mixture of **4** (1.20 g, 2.92 mmol, 1.0 equiv), 2-aminopyrimidine-5-boronic acid pinacol ester (970 mg, 4.39 mmol, 1.5 equiv), Cs₂CO₃ (3.81 g, 11.7 mmol, 4.0 equiv), water (6 mL), and dioxane (12 mL) was degassed with N₂, then Pd(dppf)Cl₂ (238 mg, 0.29 mmol, 0.1 equiv) was added, and the mixture heated at 90 °C for 5 h. The mixture was allowed to cool, then concentrated to dryness and purified by chromatography on silica gel (2–20% MeOH/EtOAc) to give **5** as a beige solid (1.07 g, 86%). ¹H NMR (400 MHz, DMSO-*d*₆) δ ppm 8.96 (s, 2H), 7.78 (s, 1H), 7.70 (d, *J* = 9.6 Hz, 1H), 6.96 (d, *J* = 6.9 Hz, 1H), 6.87–6.78 (m, 3H), 6.62 (d, *J* = 9.6 Hz, 1H), 3.52–3.42 (m, 1H), 3.30–3.21 (m, 1H), 2.17–2.08 (m, 2H), 1.90–1.79 (m, 2H), 1.38 (s, 9H), 1.32–1.21 (m, 4H). *m/z* (ES + APCI)⁺: 425 [M + H]⁺.

trans-N-{3-[2-(Pyridin-2-ylamino)pyrimidin-5-yl]imidazo[1,2-b]pyridazin-6-yl}cyclohexane-1,4-diamine 2. Compound **5** (90 mg, 0.21 mmol, 1.1 equiv), 2-chloropyridine (18 μL, 22 mg, 0.19 mmol, 1.0 equiv), and sodium *tert*-butoxide (73 mg, 0.76 mmol, 4.0 equiv) were added to a prestirred solution of Pd(OAc)₂ (4.3 mg, 0.1 equiv) and CyPF-^tBu (10.5 mg, 10 mol %) in DME (1.5 mL), and the mixture was heated at 80 °C for 3 h. The mixture was allowed to cool, diluted with CH₂Cl₂, and passed through an Isolute silica cartridge (1 g) eluting with CH₂Cl₂/MeOH (7:3). The eluent was concentrated under reduced pressure, then stirred in MeOH (3 mL) and 4 M HCl/dioxane (2 mL) for 40 min, concentrated under reduced pressure, and purified by prep-HPLC to give **2** as a white solid (5 mg, 6%). ¹H NMR (400 MHz, CD₃OD) δ ppm 9.24 (s, 2H), 8.39–8.34 (m, 1H), 8.29–8.24 (m, 1H), 7.81 (s, 1H), 7.80–7.76 (m, 1H), 7.62 (d, *J* = 10.1 Hz, 1H), 7.05–7.00 (m, 1H), 6.69 (d, *J* = 9.6 Hz, 1H), 3.73–3.63 (m, 1H), 2.90–2.80 (m, 1H), 2.31–2.22 (m, 2H), 2.07–1.98 (m, 2H), 1.50–1.30 (m, 4H). *m/z* (ES + APCI)⁺: 402 [M + H]⁺.

trans-N-{3-[2-(Phenylamino)pyrimidin-5-yl]imidazo[1,2-b]pyridazin-6-yl}cyclohexane-1,4-diamine 6. Compound **5** (90 mg,

0.21 mmol, 1.1 equiv), iodobenzene (21 μ L, 39 mg, 0.19 mmol, 1.0 equiv), and sodium *tert*-butoxide (73 mg, 0.76 mmol, 4.0 equiv) were added to a prestirred solution of Pd(OAc)₂ (4.3 mg, 0.1 equiv) and CyPF-Bu (10.5 mg, 0.1 equiv) in dioxane (1.5 mL), and the mixture was heated at 80 °C for 40 h. The mixture was allowed to cool, and 4 M HCl/dioxane (1 mL) was added and the mixture stirred for 2 h, then concentrated to dryness, and purified by prep-HPLC to give **6** as an off-white solid (15 mg, 18%). ¹H NMR (400 MHz, DMSO-*d*₆) δ ppm 9.91 (s, 1H), 9.24 (s, 2H), 7.91–7.88 (m, 1H), 7.83–7.77 (m, 2H), 7.76–7.71 (m, 1H), 7.33–7.26 (m, 2H), 7.03–6.92 (m, 2H), 6.67 (d, *J* = 9.6 Hz, 1H), 3.58–3.46 (m, 1H), 2.66–2.56 (m, 1H), 2.15–2.07 (m, 2H), 1.87–1.78 (m, 2H), 1.33–1.10 (m, 4H). *m/z* (ES + APCI)⁺: 401 [M + H]⁺.

trans-N-[3-[2-(Pyrazin-2-ylamino)pyrimidin-5-yl]imidazo[1,2-*b*]pyridazin-6-yl]cyclohexane-1,4-diamine **7**. Compound **5** (80 mg, 0.19 mmol, 1.0 equiv), 2-chloropyrazine (22 mg, 0.19 mmol, 1.0 equiv), Pd(OAc)₂ (4.3 mg, 0.1 equiv), Xantphos (11 mg, 0.1 equiv), and Cs₂CO₃ (248 mg, 0.76 mmol, 4.0 equiv) in dioxane (1 mL) under N₂ were heated at 90 °C for 10 h. The mixture was allowed to cool, and 4 M HCl/dioxane (1 mL) was added and the mixture stirred for 2 h then concentrated to dryness. Purification by prep-HPLC gave **7** as a white solid (8 mg, 10%). ¹H NMR (400 MHz, DMSO-*d*₆) δ ppm 10.52 (br. s, 1H), 9.52 (d, *J* = 1.4 Hz, 1H), 9.34 (s, 2H), 8.36–8.34 (m, 1H), 8.24 (d, *J* = 2.3 Hz, 1H), 7.97 (s, 1H), 7.77 (d, *J* = 9.6 Hz, 1H), 7.04 (d, *J* = 6.9 Hz, 1H), 6.70 (d, *J* = 9.6 Hz, 1H), 3.58–3.49 (m, 1H), 2.76–2.65 (m, 1H), 2.17–2.09 (m, 2H), 1.90–1.82 (m, 2H), 1.34–1.16 (m, 4H). *m/z* (ES + APCI)⁺: 403 [M + H]⁺.

trans-N-[3-[2-(Pyridin-3-ylamino)pyrimidin-5-yl]imidazo[1,2-*b*]pyridazin-6-yl]cyclohexane-1,4-diamine **8**. Following the method for **6** using **5** and 3-bromopyridine, we obtained **8** as an orange/brown solid (28% yield). ¹H NMR (400 MHz, DMSO-*d*₆) δ ppm 10.14–10.08 (m, 1H), 9.29 (s, 2H), 8.94 (d, *J* = 1.8 Hz, 1H), 8.28–8.24 (m, 1H), 8.19–8.16 (m, 1H), 7.93 (s, 1H), 7.75 (d, *J* = 9.6 Hz, 1H), 7.36–7.32 (m, 1H), 7.03 (d, *J* = 6.9 Hz, 1H), 6.67 (d, *J* = 9.6 Hz, 1H), 3.57–3.47 (m, 1H), 2.66–2.58 (m, 1H), 2.16–2.08 (m, 2H), 1.88–1.80 (m, 2H), 1.32–1.11 (m, 4H). *m/z* (ES + APCI)⁺: 402 [M + H]⁺.

trans-N-[3-[2-(Pyrimidin-2-ylamino)pyrimidin-5-yl]imidazo[1,2-*b*]pyridazin-6-yl]cyclohexane-1,4-diamine **9**. Following the method for **7** using **5** and 2-chloropyrimidine, we obtained **9** as a white solid (10% yield). ¹H NMR (400 MHz, DMSO-*d*₆) δ ppm 10.45 (br. s, 1H), 9.30 (s, 2H), 8.60 (d, *J* = 5.0 Hz, 2H), 7.97 (s, 1H), 7.78 (d, *J* = 9.6 Hz, 1H), 7.08–7.03 (m, 2H), 6.70 (d, *J* = 9.6 Hz, 1H), 3.60–3.50 (m, 1H), 2.82–2.73 (m, 1H), 2.18–2.09 (m, 2H), 1.92–1.84 (m, 2H), 1.34–1.20 (m, 4H). *m/z* (ES + APCI)⁺: 403 [M + H]⁺.

trans-N-[3-[2-[(3-Fluoropyridin-2-yl)amino]pyrimidin-5-yl]imidazo[1,2-*b*]pyridazin-6-yl]cyclohexane-1,4-diamine **10**. Following the method for **7** using **5** and 2-chloro-3-fluoropyridine, we obtained **10** as a yellow solid (3% yield). ¹H NMR (400 MHz, DMSO-*d*₆) δ ppm 10.04 (br. s, 1H), 9.16 (s, 2H), 8.25–8.19 (m, 1H), 7.87 (s, 1H), 7.77–7.69 (m, 2H), 7.32–7.23 (m, 1H), 6.99 (d, *J* = 6.9 Hz, 1H), 6.67 (d, *J* = 10.5 Hz, 1H), 3.57–3.44 (m, 1H), 2.65–2.56 (m, 1H), 2.14–2.03 (m, 2H), 1.86–1.76 (m, 2H), 1.31–1.08 (m, 4H). *m/z* (ES + APCI)⁺: 420 [M + H]⁺.

trans-N-[3-[2-[(3-Fluoro-5-(trifluoromethyl)pyridin-2-yl)amino]pyrimidin-5-yl]imidazo[1,2-*b*]pyridazin-6-yl]cyclohexane-1,4-diamine **11**. Following the method for **7** using 2-bromo-3-fluoro-5-(trifluoromethyl)pyridine, we obtained **11** as a yellow solid (14% yield). ¹H NMR (400 MHz, DMSO-*d*₆) δ ppm 9.26 (s, 2H), 8.61 (s, 1H), 8.25 (dd, *J* = 10.5, 1.8 Hz, 1H), 7.94 (s, 1H), 7.75 (d, *J* = 9.6 Hz, 1H), 7.03 (d, *J* = 6.9 Hz, 1H), 6.68 (d, *J* = 9.6 Hz, 1H), 3.56–3.46 (m, 1H), 2.65–2.57 (m, 1H), 2.13–2.05 (m, 2H), 1.86–1.78 (m, 2H), 1.31–1.09 (m, 4H). *m/z* (ES + APCI)⁺: 488 [M + H]⁺.

trans-N-[3-[2-[(5-Methylpyridin-2-yl)amino]pyrimidin-5-yl]imidazo[1,2-*b*]pyridazin-6-yl]cyclohexane-1,4-diamine **12**. Following the method for **7** using 2-chloro-5-methylpyridine, we obtained **12** as an off-white solid (5% yield). ¹H NMR (400 MHz, DMSO-*d*₆) δ ppm 9.92 (s, 1H), 9.26 (s, 2H), 8.17 (d, *J* = 8.7 Hz, 1H), 8.14–8.11 (m, 1H), 7.92 (s, 1H), 7.75 (d, *J* = 9.6 Hz, 1H), 7.60 (dd, *J* = 2.3, 8.7 Hz, 1H), 7.00 (d, *J* = 6.9 Hz, 1H), 6.67 (d, *J* = 9.6 Hz, 1H), 3.57–3.47

(m, 1H), 2.65–2.56 (m, 1H), 2.25 (s, 3H), 2.14–2.07 (m, 2H), 1.86–1.79 (m, 2H), 1.32–1.13 (m, 4H). *m/z* (ES + APCI)⁺: 416 [M + H]⁺.

tert-Butyl [trans-4-[(3-[2-(methylsulfonyl)pyrimidin-5-yl]imidazo[1,2-*b*]pyridazin-6-yl)amino]cyclohexyl]carbamate **13**. Following the method for **5** using 2-(thiomethyl)pyrimidine-5-boronic acid, we obtained **13** as a pale yellow solid (90% yield). ¹H NMR (400 MHz, DMSO-*d*₆) δ ppm 9.38 (s, 2H), 8.03 (s, 1H), 7.77 (d, *J* = 9.6 Hz, 1H), 7.09 (br. d, *J* = 6.9 Hz, 1H), 6.83 (br. d, *J* = 8.2 Hz, 1H), 6.71 (d, *J* = 9.6 Hz, 1H), 3.53–3.47 (m, 1H), 3.31–3.26 (m, 1H), 2.58 (s, 3H), 2.15–2.11 (m, 2H), 1.87–1.82 (m, 2H), 1.39 (s, 9H), 1.35–1.23 (m, 4H). *m/z* (ES + APCI)⁺: 456 [M + H]⁺.

trans-N-[3-[2-[(Pyridin-3-ylmethyl)amino]pyrimidin-5-yl]imidazo[1,2-*b*]pyridazin-6-yl]cyclohexane-1,4-diamine **14**. Compound **13** (2.00 g, 4.39 mmol, 1.0 equiv) in CH₂Cl₂ (60 mL) was treated with mCPBA (2.38 g, 9.66 mmol, 2.2 equiv) and stirred at rt for 2 h. The mixture was diluted with saturated aqueous Na₂SO₃ (20 mL) and CH₂Cl₂ (50 mL) and washed with saturated aqueous NaHCO₃ (80 mL). The aqueous layer was extracted with CH₂Cl₂ (50 mL), then the combined organic layers were washed with brine (60 mL), dried, and concentrated to give an orange solid (2.1 g, 98%). ¹H NMR (400 MHz, DMSO-*d*₆) δ ppm 9.80 (s, 2H), 8.30 (s, 1H), 7.85 (d, *J* = 9.6 Hz, 1H), 7.24 (br. d, *J* = 6.9 Hz, 1H), 6.85 (br. d, *J* = 8.2 Hz, 1H), 6.82 (d, *J* = 10.3 Hz, 1H), 3.60–3.52 (m, 1H), 3.44 (s, 3H), 3.33–3.25 (m, 1H), 2.17–2.13 (m, 2H), 1.88–1.83 (m, 2H), 1.39 (s, 9H), 1.37–1.23 (m, 4H). A solution of the intermediate (60 mg, 0.12 mmol, 1.0 equiv) in dioxane (2 mL) was treated with 1-(pyridin-3-yl)methanamine (54 mg, 0.49 mmol, 4.0 equiv) and stirred at reflux for 4 h. Concentration under reduced pressure, purification by prep-HPLC, and treatment with 4 M HCl/dioxane (1 mL) followed by elution through an Isolute aminopropyl cartridge gave **14** as an off-white solid (12 mg, 24%). ¹H NMR (400 MHz, DMSO-*d*₆) δ ppm 9.02 (br. s, 2H), 8.58 (d, *J* = 1.8 Hz, 1H), 8.48–8.38 (m, 1H), 8.08 (t, *J* = 6.4 Hz, 1H), 7.78–7.68 (m, 3H), 7.43–7.27 (m, 1H), 6.94 (d, *J* = 6.9 Hz, 1H), 6.62 (d, *J* = 9.6 Hz, 1H), 4.55 (d, *J* = 6.4 Hz, 2H), 3.53–3.41 (m, 1H), 2.64–2.55 (m, 1H), 2.13–2.01 (m, 2H), 1.88–1.75 (m, 2H), 1.33–1.08 (m, 4H). *m/z* (ES + APCI)⁺: 416 [M + H]⁺.

trans-N-[3-[2-[(Pyridin-2-ylmethyl)amino]pyrimidin-5-yl]imidazo[1,2-*b*]pyridazin-6-yl]cyclohexane-1,4-diamine **15**. Following the method for **14** using 1-(pyridin-2-yl)methanamine, we obtained **15** as an off-white solid (27% yield). ¹H NMR (400 MHz, DMSO-*d*₆) δ ppm 9.00 (br. s, 2H), 8.50 (dt, *J* = 0.9, 2.5 Hz, 1H), 8.04–7.96 (m, 1H), 7.78–7.67 (m, 3H), 7.32 (d, *J* = 7.8 Hz, 1H), 7.24 (ddd, *J* = 0.9, 4.8, 7.6 Hz, 1H), 6.93 (d, *J* = 6.9 Hz, 1H), 6.62 (d, *J* = 9.6 Hz, 1H), 4.64 (d, *J* = 6.4 Hz, 2H), 3.55–3.40 (m, 1H), 2.66–2.56 (m, 1H), 2.18–2.02 (m, 2H), 1.89–1.76 (m, 2H), 1.31–1.06 (m, 4H). *m/z* (ES + APCI)⁺: 416 [M + H]⁺.

trans-N-[3-[2-[(1-Methyl-1H-pyrazol-3-yl)methyl]amino]pyrimidin-5-yl]imidazo[1,2-*b*]pyridazin-6-yl]cyclohexane-1,4-diamine **16**. Following the method for **14** using 1-(1-methyl-1H-pyrazol-3-yl)methanamine, we obtained **16** as an off-white solid (11% yield). ¹H NMR (400 MHz, DMSO-*d*₆) δ ppm 9.00 (br. s, 2H), 7.81–7.65 (m, 3H), 7.55 (d, *J* = 2.3 Hz, 1H), 6.93 (d, *J* = 6.9 Hz, 1H), 6.62 (d, *J* = 9.6 Hz, 1H), 6.13 (d, *J* = 2.3 Hz, 1H), 4.47 (d, *J* = 6.0 Hz, 2H), 3.77 (s, 3H), 3.55–3.40 (m, 1H), 2.64–2.54 (m, 1H), 2.15–2.03 (m, 2H), 1.89–1.74 (m, 2H), 1.37–1.08 (m, 4H). *m/z* (ES + APCI)⁺: 419 [M + H]⁺.

tert-Butyl 4-[(3-bromoimidazo[1,2-*b*]pyridazin-6-yl)amino]piperidine-1-carboxylate **17**. A solution of **3** (3.00 g, 12.9 mmol 1.0 equiv) in NMP (15 mL) was treated with *tert*-butyl 4-aminopiperidine-1-carboxylate (5.10 g, 25.8 mmol, 2.0 equiv), DIPEA (5.60 mL, 32.3 mmol, 2.5 equiv), and heated at 130 °C for 5 h. The reaction mixture was diluted with CH₂Cl₂ (100 mL) and washed with deionized water (3 \times 150 mL). The separated organic layer was concentrated under reduced pressure and column chromatography (10–80% EtOAc/pet ether) to give **17** as a brown solid (3.01 g, 59%). ¹H NMR (400 MHz, DMSO-*d*₆) δ ppm 7.71 (d, *J* = 9.6 Hz, 1H), 7.48 (s, 1H), 7.10 (br. d, *J* = 7.3 Hz, 1H), 6.68 (d, *J* = 10.1 Hz, 1H), 3.87–3.82 (m, 3H), 3.02–2.93 (m, 2H), 2.02–1.98 (m, 2H), 1.41 (s, 9H), 1.40–1.31 (m, 2H). *m/z* (ES + APCI)⁺: 396/398 [M + H]⁺.

tert-Butyl 4-[[3-(2-aminopyrimidin-5-yl)imidazo[1,2-*b*]pyridazin-6-yl]amino]piperidine-1-carboxylate **18**. Following the procedure for **5** using **17**, we obtained **18** as a beige solid (100% yield). ¹H NMR (400 MHz, DMSO-*d*₆) δ ppm 8.95 (s, 2H), 7.79 (s, 1H), 7.74 (d, *J* = 9.6 Hz, 1H), 7.06 (d, *J* = 6.4 Hz, 1H), 6.85 (s, 2H), 6.65 (d, *J* = 9.6 Hz, 1H), 3.93–3.83 (m, 2H), 3.80–3.71 (m, 1H), 3.01–2.88 (m, 2H), 2.06–2.00 (m, 2H), 1.42 (s, 9H), 1.39–1.31 (m, 2H). *m/z* (ES + APCI)⁺: 411 [M + H]⁺.

3-[2-[(3-Fluoropyridin-2-yl)amino]pyrimidin-5-yl]-*N*-(1-methylpiperidin-4-yl)imidazo[1,2-*b*]pyridazin-6-amine **19**. (a) To a mixture of **18** (100 mg, 0.24 mmol, 1.0 equiv), 2-chloro-3-fluoropyridine (28 mg, 0.30 mmol, 1.2 equiv) and Cs₂CO₃ (316 mg, 0.97 mmol, 4.0 equiv) in dioxane (3.0 mL) was added Pd(OAc)₂ (6 mg, 0.1 equiv) and Xantphos (16 mg, 0.1 equiv). The reaction mixture was heated in the microwave at 130 °C for 50 min, diluted with CH₂Cl₂ (20 mL), and washed with deionized water (20 mL). The organic was separated and treated with 4 M HCl/dioxane (2 mL) and methanol (5 mL). The product was purified by prep-HPLC give a white solid (24 mg, 24%). ¹H NMR (400 MHz, DMSO-*d*₆) δ ppm 9.99 (s, 1H), 9.13 (s, 2H), 8.23 (td, *J* = 4.6, 1.4 Hz, 1H), 7.87 (s, 1H), 7.77 (d, *J* = 9.6 Hz, 1H), 7.76–7.70 (m, 1H), 7.29 (ddd, *J* = 8.4, 4.9, 3.7 Hz, 1H), 7.10 (d, *J* = 6.9 Hz, 1H), 6.69 (d, *J* = 9.6 Hz, 1H), 3.83–3.61 (m, 1H), 3.13–3.03 (m, 2H), 2.78–2.63 (m, 2H), 2.14–1.94 (m, 2H), 1.59–1.31 (m, 2H). *m/z* (ES + APCI)⁺: 406 [M + H]⁺. (b) To a solution of 3-[2-[(3-fluoropyridin-2-yl)amino]pyrimidin-5-yl]-*N*-(piperidin-4-yl)imidazo[1,2-*b*]pyridazin-6-amine (30 mg, 0.07 mmol, 1.0 equiv) in THF (0.5 mL) was added formaldehyde (37% aq., 6 μL, 0.07 mmol, 1.0 equiv), AcOH (8 μL, 0.148 mmol, 2.0 equiv), and sodium triacetoxyborohydride (31 mg, 0.015 mmol, 2.0 equiv). The reaction mixture was stirred for 2 h at rt and concentrated under reduced pressure. Purification by prep-HPLC gave **19** as an off-white solid (12 mg, 39%). ¹H NMR (400 MHz, DMSO-*d*₆) δ ppm 10.01 (d, *J* = 4.1 Hz, 1H), 9.15–9.12 (m, 2H), 8.24–8.21 (m, 1H), 7.87 (s, 1H), 7.77–7.69 (m, 2H), 7.29 (ddd, *J* = 8.1, 4.7, 3.7 Hz, 1H), 7.09–7.03 (m, 1H), 6.69 (d, *J* = 9.6 Hz, 1H), 3.64–3.50 (m, 1H), 2.82–2.70 (m, 2H), 2.18 (s, 3H), 2.09–1.90 (m, 4H), 1.54–1.31 (m, 2H). *m/z* (ES + APCI)⁺: 420 [M + H]⁺.

tert-Butyl 4-[[3-(6-aminopyridin-3-yl)imidazo[1,2-*b*]pyridazin-6-yl]amino]piperidine-1-carboxylate **20**. Following the method for **5** using **17** and 2-aminopyridine-5-boronic acid pinacol ester, we obtained **20** as an off-white solid (91% yield). ¹H NMR (400 MHz, DMSO-*d*₆) δ ppm 8.69 (d, *J* = 1.8 Hz, 1H), 8.07 (dd, *J* = 2.3, 8.7 Hz, 1H), 7.74–7.65 (m, 2H), 7.00 (d, *J* = 6.4 Hz, 1H), 6.61 (d, *J* = 10.1 Hz, 1H), 6.54 (dd, *J* = 0.9, 8.7 Hz, 1H), 6.12 (s, 2H), 3.96–3.83 (m, 2H), 3.82–3.68 (m, 1H), 3.04–2.84 (m, 2H), 2.11–1.96 (m, 2H), 1.47–1.27 (m, 11H). *m/z* (ES + APCI)⁺: 410 [M + H]⁺.

3-[6-[(3-Fluoropyridin-2-yl)amino]pyridin-3-yl]-*N*-(piperidin-4-yl)imidazo[1,2-*b*]pyridazin-6-amine **21**. Following the method for **7** using **20**, we obtained an off-white solid (33% yield). ¹H NMR (400 MHz, DMSO-*d*₆) δ ppm 9.30 (br. s, 1H), 9.13–9.01 (m, 1H), 8.42 (dd, *J* = 2.5, 8.9 Hz, 1H), 8.19–8.09 (m, 1H), 8.09–8.04 (m, 1H), 7.87 (s, 1H), 7.74 (d, *J* = 9.6 Hz, 1H), 7.65 (ddd, *J* = 1.4, 8.0, 11.2 Hz, 1H), 7.09–6.94 (m, 2H), 6.68 (d, *J* = 10.1 Hz, 1H), 3.77–3.59 (m, 1H), 3.06–2.89 (m, 2H), 2.63–2.52 (m, 2H), 2.07–1.87 (m, 2H), 1.43–1.20 (m, 2H). *m/z* (ES + APCI)⁺: 405 [M + H]⁺. This was then treated following the method for **19b**, which gave **21** as a yellow solid (22 mg, 76%). ¹H NMR (400 MHz, DMSO-*d*₆) δ ppm 9.31 (s, 1H), 9.07 (d, *J* = 2.3 Hz, 1H), 8.45–8.36 (m, 1H), 8.15–8.09 (m, 1H), 8.06 (d, *J* = 8.2 Hz, 1H), 7.87 (s, 1H), 7.75 (d, *J* = 9.6 Hz, 1H), 7.65 (ddd, *J* = 1.4, 8.0, 11.2 Hz, 1H), 7.07–6.94 (m, 2H), 6.69 (d, *J* = 9.6 Hz, 1H), 3.60 (d, *J* = 6.4 Hz, 1H), 2.81–2.70 (m, 2H), 2.19 (s, 3H), 2.12–1.97 (m, 4H), 1.60–1.38 (m, 2H). *m/z* (ES + APCI)⁺: 419 [M + H]⁺.

N-(3-Fluoropyridin-2-yl)-5-(6-methylimidazo[1,2-*b*]pyridazin-3-yl)pyrimidin-2-amine **22**. (a) To a solution of 3-amino-6-methylpyridazine (5.0 g, 45.8 mmol, 1.0 equiv) in butan-1-ol (10 mL) was added 50% chloroacetaldehyde in water (6.4 mL, 50.4 mmol, 1.1 equiv). The reaction mixture was heated at reflux for 4 h, then concentrated under reduced pressure, and purification by column chromatography (0–10% MeOH in CH₂Cl₂) gave 6-methylimidazo[1,2-*b*]pyridazine as a beige solid (4.2 g, 69%). ¹H NMR (400 MHz, DMSO-*d*₆) δ ppm 8.62

(d, *J* = 2.3 Hz, 1H), 8.41 (d, *J* = 9.2 Hz, 1H), 8.32 (d, *J* = 2.3 Hz, 1H), 7.75 (d, *J* = 9.2 Hz, 1H), 2.65 (s, 3H). (b) To a solution of 6-methylimidazo[1,2-*b*]pyridazine (4.0 g, 30.0 mmol, 1.0 equiv) in MeCN (40 mL) was added *N*-bromosuccinimide (5.9 g, 33.0 mmol, 1.1 equiv) portionwise. The reaction mixture was stirred overnight at rt, then concentrated under reduced pressure, dissolved in CH₂Cl₂ (200 mL), and washed with deionized water (3 × 200 mL). The organic phase was separated and dried (MgSO₄), and purification by column chromatography (0–10% MeOH in CH₂Cl₂) gave 3-bromo-6-methylimidazo[1,2-*b*]pyridazine as a red solid (2.0 g, 31%). ¹H NMR (400 MHz, DMSO-*d*₆) δ ppm 8.05 (d, *J* = 9.2 Hz, 1H), 7.83 (s, 1H), 7.21 (d, *J* = 9.2 Hz, 1H), 2.58 (s, 3H). (c) To a solution of 3-bromo-6-methylimidazo[1,2-*b*]pyridazine (2.0 g, 9.43 mmol, 1.0 equiv) in dioxane (10 mL) was added 5-(4,4,5,5-tetramethyl-1,3,2-dioxaborolan-2-yl)pyrimidin-2-amine (2.5 g, 11.3 mmol, 1.2 equiv), bis(*tert*-butyl(4-dimethylaminophenyl)phosphine)dichloropalladium(II) (332 mg, 0.47 mmol, 0.05 equiv), and 2 M sodium carbonate (18.8 mL, 37.7 mmol, 4.0 equiv). The reaction mixture was heated at 80 °C for 6 h, concentrated under reduced pressure, and the residue taken up in CH₂Cl₂ (100 mL). The organic phase was washed with deionized water (3 × 100 mL) and dried (MgSO₄), and purification by column chromatography (0–10% MeOH in CH₂Cl₂) gave 5-(6-methylimidazo[1,2-*b*]pyridazin-3-yl)pyrimidin-2-amine as an off-white solid (205 mg, 10%). ¹H NMR (400 MHz, DMSO-*d*₆) δ ppm 8.92 (s, 2H), 8.12–8.00 (m, 2H), 7.16 (d, *J* = 9.2 Hz, 1H), 6.93 (s, 2H), 2.57 (s, 3H). *m/z* (ES + APCI)⁺: 227 [M + H]⁺. (d) A mixture of 5-(6-methylimidazo[1,2-*b*]pyridazin-3-yl)pyrimidin-2-amine (95 mg, 0.42 mmol, 1.0 equiv), 2-chloro-3-fluoropyridine (82 mg, 0.63 mmol, 1.5 equiv), Pd(OAc)₂ (19 mg, 0.08 mmol, 0.2 equiv), Xantphos (49 mg, 0.08 mmol, 0.2 equiv), and Cs₂CO₃ (547 mg, 1.68 mmol, 4.0 equiv) in dioxane (3 mL) was heated at 120 °C for 2 h. The reaction mixture was diluted with CH₂Cl₂ (100 mL) and washed with deionized water (3 × 100 mL). Purification by column chromatography (2–20% MeOH in CH₂Cl₂) gave **22** as a yellow solid (36 mg, 28%). ¹H NMR (400 MHz, DMSO-*d*₆) δ ppm 10.06 (s, 1H), 9.16 (s, 2H), 8.25 (td, *J* = 1.3, 4.7 Hz, 1H), 8.19 (s, 1H), 8.10 (d, *J* = 9.2 Hz, 1H), 7.76 (ddd, *J* = 10.5, 8.2, 1.4 Hz, 1H), 7.31 (ddd, *J* = 3.9, 4.8, 8.2 Hz, 1H), 7.20 (d, *J* = 9.6 Hz, 1H), 2.58 (s, 3H). *m/z* (ES + APCI)⁺: 322 [M + H]⁺.

N-(3-Fluoropyridin-2-yl)-5-[6-(piperazin-1-yl)imidazo[1,2-*b*]pyridazin-3-yl]pyrimidin-2-amine **23**. (a) Following the method for **17** using *tert*-butyl piperazine-1-carboxylate, we obtained *tert*-butyl 4-(3-bromoimidazo[1,2-*b*]pyridazin-6-yl)piperazine-1-carboxylate as a yellow solid (33% yield). ¹H NMR (400 MHz, DMSO-*d*₆) δ ppm 7.91 (d, *J* = 10.1 Hz, 1H), 7.62 (s, 1H), 7.24 (d, *J* = 10.1 Hz, 1H), 3.62–3.42 (m, 8H), 1.43 (s, 9H). *m/z* (ES + APCI)⁺: 382/384 [M + H]⁺. (b) Following the method for **5** using *tert*-butyl 4-(3-bromoimidazo[1,2-*b*]pyridazin-6-yl)piperazine-1-carboxylate, we obtained *tert*-butyl 4-[3-(2-aminopyrimidin-5-yl)imidazo[1,2-*b*]pyridazin-6-yl]piperazine-1-carboxylate as a brown solid (902 mg, 77%). ¹H NMR (400 MHz, DMSO-*d*₆) δ ppm 8.91 (s, 2H), 7.93 (d, *J* = 9.6 Hz, 1H), 7.90 (s, 1H), 7.20 (d, *J* = 10.1 Hz, 1H), 6.86 (s, 2H), 3.49 (br. s, 8H), 1.42 (s, 9H). *m/z* (ES + APCI)⁺: 397 [M + H]⁺. (c) To a solution of *tert*-butyl 4-[3-(2-aminopyrimidin-5-yl)imidazo[1,2-*b*]pyridazin-6-yl]piperazine-1-carboxylate (300 mg, 0.76 mmol, 1.0 equiv), 2-chloro-3-fluoropyridine (15 mg, 1.14 mmol, 1.5 equiv), and Cs₂CO₃ (990 mg, 3.03 mmol, 4.0 equiv) in dioxane (10 mL) was added Pd(OAc)₂ (50 mg, 0.23 mmol, 0.3 equiv) and Xantphos (130 mg, 0.23 mmol, 0.3 equiv). The reaction mixture was heated at reflux for 2 h, diluted with CH₂Cl₂ (100 mL), and washed with deionized water (3 × 100 mL). The combined organics were dried and concentrated under reduced pressure. Purification by column chromatography (2–20% MeOH/DCM) gave 112 mg of Boc-protected intermediate, which was treated with 4 M HCl in dioxane (2 mL). The reaction mixture was basified with triethylamine and concentrated under reduced pressure. Purification by column chromatography (5–30% MeOH/DCM) gave **23** as an off-white solid (45 mg, 15%). ¹H NMR (400 MHz, DMSO-*d*₆) δ ppm 10.00 (s, 1H), 9.14 (s, 2H), 8.24 (td, *J* = 4.6, 1.4 Hz, 1H), 8.00 (s, 1H), 7.91 (d, *J* = 9.6 Hz, 1H), 7.75 (ddd, *J* = 10.5, 8.2, 1.4 Hz, 1H), 7.30 (ddd, *J* =

8.2, 4.6, 3.7 Hz, 1H), 7.22 (d, $J = 10.1$ Hz, 1H), 3.47–3.37 (m, 4H), 2.90–2.78 (m, 4H). m/z (ES + APCI)⁺: 392 [M + H]⁺.

N-(3-Fluoropyridin-2-yl)-5-[6-(4-methylpiperazin-1-yl)imidazo[1,2-*b*]pyridazin-3-yl]pyrimidin-2-amine **24**. Following the method for **19b** using **23**, we obtained **24** as an off-white solid (41% yield). ¹H NMR (400 MHz, DMSO-*d*₆) δ ppm 10.00 (s, 1H), 9.13 (s, 2H), 8.24 (td, $J = 4.9, 1.2$ Hz, 1H), 8.00 (s, 1H), 7.93 (d, $J = 10.1$ Hz, 1H), 7.75 (ddd, $J = 10.5, 8.0, 1.6$ Hz, 1H), 7.30 (ddd, $J = 8.1, 4.7, 3.7$ Hz, 1H), 7.25 (d, $J = 10.1$ Hz, 1H), 3.59–3.44 (m, 4H), 2.48–2.39 (m, 4H), 2.22 (s, 3H). m/z (ES + APCI)⁺: 406 [M + H]⁺.

(*R,S*)-3-{2-[(3-Fluoropyridin-2-yl)amino]pyrimidin-5-yl}-*N*-(pyrrolidin-3-yl)imidazo[1,2-*b*]pyridazin-6-amine **25**. (a) Compound **3** (1.00 g, 4.30 mmol, 1.0 equiv), (*R,S*)-3-amino-1-*N*-Boc-pyrrolidine (2.00 g, 2.5 equiv), and NMP (4 mL) were heated at 140 °C for 16 h. The mixture was diluted with EtOAc (80 mL) and washed with water (60 mL). The aqueous layer was extracted with EtOAc (30 mL), and the combined organic layers were dried and concentrated under reduced pressure. Purification by silica gel chromatography (0.2–3.5% MeOH/EtOAc) gave (*R,S*)-*tert*-butyl 3-[(3-bromoimidazo[1,2-*b*]pyridazin-6-yl)amino]pyrrolidine-1-carboxylate as a brown-yellow solid (588 mg, 36%). ¹H NMR (400 MHz, DMSO-*d*₆) δ ppm 7.73 (d, $J = 9.6$ Hz, 1H), 7.50 (s, 1H), 7.45–7.38 (m, 1H), 6.71 (d, $J = 9.6$ Hz, 1H), 4.31–4.20 (m, 1H), 3.73–3.58 (m, 1H), 3.42–3.13 (m, 3H), 2.21–2.12 (m, 1H), 1.95–1.83 (m, 1H), 1.43–1.36 (m, 9H). (b) Following the method for **5** using (*R,S*)-*tert*-butyl 3-[(3-bromoimidazo[1,2-*b*]pyridazin-6-yl)amino]pyrrolidine-1-carboxylate, we obtained (*R,S*)-*tert*-butyl 3-[(3-(2-aminopyrimidin-5-yl)imidazo[1,2-*b*]pyridazin-6-yl)amino]pyrrolidine-1-carboxylate as a pale yellow solid (272 mg, 45%). ¹H NMR (400 MHz, DMSO-*d*₆) δ ppm 8.94 (d, $J = 7.8$ Hz, 2H), 7.81–7.73 (m, 2H), 7.35–7.28 (m, 1H), 6.84 (br. s, 2H), 6.66 (d, $J = 9.6$ Hz, 1H), 4.26–4.19 (m, 1H), 3.68–3.46 (m, 1H), 3.41–3.34 (m, 2H), 3.30–3.18 (m, 1H), 2.21–2.06 (m, 1H), 2.04–1.87 (m, 1H), 1.39 (d, $J = 12.8$ Hz, 9H). m/z (ES)⁺: 397 [M + H]⁺. (c) (*R,S*)-*tert*-Butyl 3-[(3-(2-aminopyrimidin-5-yl)imidazo[1,2-*b*]pyridazin-6-yl)amino]pyrrolidine-1-carboxylate (100 mg, 0.25 mmol, 1.0 equiv), 2-chloro-3-fluoropyridine (35 μ L, 46 mg, 0.35 mmol, 1.4 equiv), Pd(OAc)₂ (11 mg, 0.2 equiv), Xantphos (0.2 equiv), and Cs₂CO₃ (326 mg, 1.00 mmol, 4.0 equiv) in dioxane (1.5 mL) were heated at 100 °C for 8 h. The mixture was allowed to cool and concentrated under reduced pressure, and purification by silica chromatography (1–10% MeOH/EtOAc) gave (*R,S*)-*tert*-butyl 3-[(3-{2-[(3-fluoropyridin-2-yl)amino]pyrimidin-5-yl}imidazo[1,2-*b*]pyridazin-6-yl)amino]pyrrolidine-1-carboxylate as a pale yellow solid (68 mg, 55%). ¹H NMR (400 MHz, DMSO-*d*₆) δ ppm 9.99 (br. s, 1H), 9.17–9.08 (m, 2H), 8.25–8.20 (m, 1H), 7.90 (s, 1H), 7.81 (d, $J = 10.1$ Hz, 1H), 7.77–7.69 (m, 1H), 7.41–7.34 (m, 1H), 7.33–7.24 (m, 1H), 6.72 (d, $J = 10.1$ Hz, 1H), 4.30–4.20 (m, 1H), 3.71–3.46 (m, 1H), 3.40–3.35 (m, 2H), 3.30–3.15 (m, 1H), 2.20–2.08 (m, 1H), 2.02–1.92 (m, 1H), 1.43–1.31 (m, 9H). m/z (ES)⁺: 397 [M + H]⁺. (d) (*R,S*)-*tert*-Butyl 3-[(3-{2-[(3-fluoropyridin-2-yl)amino]pyrimidin-5-yl}imidazo[1,2-*b*]pyridazin-6-yl)amino]pyrrolidine-1-carboxylate (67 mg, 0.14 mmol, 1.0 equiv) was stirred with 4 M HCl/dioxane (1.5 mL) and MeOH (1.5 mL) for 5 h. The mixture was concentrated under reduced pressure, then dissolved in MeOH/CH₂Cl₂ and eluted through an Isolute aminopropyl cartridge (1 g), which gave **25** as a beige solid (52 mg, 98%). ¹H NMR (400 MHz, DMSO-*d*₆) δ ppm 9.99 (br. s, 1H), 9.20–9.12 (m, 2H), 8.26–8.20 (m, 1H), 7.89 (s, 1H), 7.78–7.71 (m, 2H), 7.32–7.26 (m, 1H), 7.23 (d, $J = 6.0$ Hz, 1H), 6.69 (d, $J = 9.6$ Hz, 1H), 4.16–4.08 (m, 1H), 3.10 (dd, $J = 11.4, 6.4$ Hz, 1H), 2.95–2.72 (m, 3H), 2.10–2.00 (m, 1H), 1.73–1.63 (m, 1H). m/z (ES)⁺: 392 [M + H]⁺.

(*R,S*)-3-{2-[(3-Fluoropyridin-2-yl)amino]pyrimidin-5-yl}-*N*-(1-methylpyrrolidin-3-yl)imidazo[1,2-*b*]pyridazin-6-amine **26**. Following the method for **19b** using **25**, we obtained **26** as a white solid (37% yield). ¹H NMR (400 MHz, CD₃OD) δ ppm 9.15 (s, 2H), 8.19 (d, $J = 5.0$ Hz, 1H), 7.82 (s, 1H), 7.71–7.59 (m, 2H), 7.26–7.19 (m, 1H), 6.76 (d, $J = 9.6$ Hz, 1H), 4.46–4.37 (m, 1H), 3.27–3.20 (m, 1H), 3.14–3.03 (m, 1H), 3.01–2.93 (m, 1H), 2.92–2.83 (m, 1H), 2.59 (s, 3H), 2.55–2.42 (m, 1H), 2.03–1.91 (m, 1H). m/z (ES)⁺: 406 [M + H]⁺.

3-{2-[(3-Fluoropyridin-2-yl)amino]pyrimidin-5-yl}-*N*-[2-(morpholin-4-yl)ethyl]imidazo[1,2-*b*]pyridazin-6-amine **27**. (a) Following the method for **17** using 2-(morpholin-4-yl)ethanamine, we obtained 3-bromo-*N*-[2-(morpholin-4-yl)ethyl]imidazo[1,2-*b*]pyridazin-6-amine as a yellow oil (41% yield). ¹H NMR (400 MHz, DMSO-*d*₆) δ ppm 7.69 (d, $J = 9.6$ Hz, 1H), 7.47 (s, 1H), 7.09 (t, $J = 5.5$ Hz, 1H), 6.74 (d, $J = 9.6$ Hz, 1H), 3.64–3.49 (m, 4H), 3.45–3.36 (m, 2H), 2.54 (t, $J = 6.6$ Hz, 2H), 2.48–2.39 (m, 4H). m/z (ES + APCI)⁺: 326/328 [M + H]⁺. (b) Following the method for **5** using 3-bromo-*N*-[2-(morpholin-4-yl)ethyl]imidazo[1,2-*b*]pyridazin-6-amine, we obtained 3-(2-aminopyrimidin-5-yl)-*N*-[2-(morpholin-4-yl)ethyl]imidazo[1,2-*b*]pyridazin-6-amine as an off-white solid (91% yield). ¹H NMR (400 MHz, DMSO-*d*₆) δ ppm 8.93 (s, 2H), 7.76 (s, 1H), 7.71 (d, $J = 9.6$ Hz, 1H), 7.03 (t, $J = 5.3$ Hz, 1H), 6.83 (s, 2H), 6.70 (d, $J = 9.6$ Hz, 1H), 3.58 (t, $J = 4.4$ Hz, 4H), 3.43–3.31 (m, 2H), 2.55 (t, $J = 6.6$ Hz, 2H), 2.47–2.34 (m, 4H). m/z (ES + APCI)⁺: 341 [M + H]⁺. (c) Following the method for **25c** using 3-(2-aminopyrimidin-5-yl)-*N*-[2-(morpholin-4-yl)ethyl]imidazo[1,2-*b*]pyridazin-6-amine with purification by prep-HPLC, we obtained **27** as an off-white solid (32% yield). ¹H NMR (400 MHz, DMSO-*d*₆) δ ppm 9.97 (s, 1H), 9.16 (s, 2H), 8.23 (td, $J = 4.6, 1.4$ Hz, 1H), 7.88 (s, 1H), 7.79–7.69 (m, 2H), 7.30 (ddd, $J = 8.2, 4.6, 3.7$ Hz, 1H), 7.09 (t, $J = 5.5$ Hz, 1H), 6.74 (d, $J = 9.6$ Hz, 1H), 3.59–3.49 (m, 4H), 3.44–3.34 (m, 2H), 2.54 (t, $J = 6.6$ Hz, 2H), 2.47–2.35 (m, 4H). m/z (ES + APCI)⁺: 436 [M + H]⁺.

3-{2-[(3-Fluoropyridin-2-yl)amino]pyrimidin-5-yl}-*N*-[2-(4-methylpiperazin-1-yl)ethyl]imidazo[1,2-*b*]pyridazin-6-amine **28**. (a) Following the method for **17** using 1-(2-aminoethyl)-4-methylpiperazine, we obtained 3-bromo-*N*-[2-(4-methylpiperazin-1-yl)ethyl]imidazo[1,2-*b*]pyridazin-6-amine as a brown solid (40% yield). ¹H NMR (400 MHz, DMSO-*d*₆) δ ppm 7.68 (d, $J = 9.6$ Hz, 1H), 7.47 (s, 1H), 7.05 (t, $J = 5.3$ Hz, 1H), 6.74 (d, $J = 9.6$ Hz, 1H), 3.42–3.34 (m, 2H), 2.57–2.51 (m, 2H), 2.50–2.21 (m, 8H), 2.14 (s, 3H). m/z (ES + APCI)⁺: 339/341 [M + H]⁺. (b) Following the method for **5** using 3-bromo-*N*-[2-(4-methylpiperazin-1-yl)ethyl]imidazo[1,2-*b*]pyridazin-6-amine, we obtained an off-white solid (68% yield). ¹H NMR (400 MHz, DMSO-*d*₆) δ ppm 8.93 (s, 2H), 7.76 (s, 1H), 7.72 (d, $J = 10.1$ Hz, 1H), 7.29–7.05 (m, 1H), 6.83 (s, 2H), 6.71 (d, $J = 9.6$ Hz, 1H), 3.45–3.35 (m, 2H), 3.02–2.52 (m, 13H). m/z (ES + APCI)⁺: 354 [M + H]⁺. (c) Following the method for **25c** using 3-(2-aminopyrimidin-5-yl)-*N*-[2-(4-methylpiperazin-1-yl)ethyl]imidazo[1,2-*b*]pyridazin-6-amine, we obtained **28** after purification by prep-HPLC as an off-white solid (11% yield). ¹H NMR (400 MHz, CD₃OD) δ ppm 9.16 (s, 2H), 8.19 (d, $J = 4.6$ Hz, 1H), 7.79 (s, 1H), 7.68–7.59 (m, 2H), 7.23 (ddd, $J = 8.1, 4.7, 3.7$ Hz, 1H), 6.73 (d, $J = 9.6$ Hz, 1H), 3.51 (t, $J = 6.9$ Hz, 2H), 2.69–2.63 (m, 2H), 2.72–2.36 (m, 8H), 2.29 (s, 3H). m/z (ES + APCI)⁺: 449 [M + H]⁺.

3-{2-[(3-Fluoropyridin-2-yl)amino]pyrimidin-5-yl}-*N*-[2-(pyrrolidin-1-yl)ethyl]imidazo[1,2-*b*]pyridazin-6-amine **29**. (a) 3-Bromo-6-chloro-imidazo[1,2-*b*]pyridazine (500 mg, 2.15 mmol, 1.0 equiv), 1,2-aminoethylpyrrolidine (682 μ L, 614 mg, 5.38 mmol, 2.5 equiv), and NMP (3 mL) were heated at 170 °C under microwave irradiation for 60 min. The mixture was diluted with EtOAc (60 mL) and washed with water (50 mL). The aqueous layer was basified to pH 10 with 2 M NaOH (aq.), extracted with EtOAc (40 mL), and the combined organic layers were dried (MgSO₄) and concentrated under reduced pressure. Purification by silica gel chromatography (2–20% MeOH/EtOAc with 1% conc. aqueous ammonia) gave 3-bromo-*N*-[2-(pyrrolidin-1-yl)ethyl]imidazo[1,2-*b*]pyridazin-6-amine as a yellow solid (450 mg, 68%). ¹H NMR (400 MHz, DMSO-*d*₆) δ ppm 7.67 (d, $J = 9.6$ Hz, 1H), 7.46 (s, 1H), 7.11 (t, $J = 5.3$ Hz, 1H), 6.75 (d, $J = 9.6$ Hz, 1H), 3.42–3.35 (m, 2H), 2.66 (t, $J = 6.6$ Hz, 2H), 2.54–2.49 (m, 4H), 1.72–1.65 (m, 4H). m/z (ES + APCI)⁺: 310/312 [M + H]⁺. (b) Following the procedure for **5** using 3-bromo-*N*-[2-(pyrrolidin-1-yl)ethyl]imidazo[1,2-*b*]pyridazin-6-amine, we obtained 3-(2-aminopyrimidin-5-yl)-*N*-[2-(pyrrolidin-1-yl)ethyl]imidazo[1,2-*b*]pyridazin-6-amine as an off-white solid (91% yield). ¹H NMR (400 MHz, DMSO-*d*₆) δ ppm 8.93 (s, 2H), 7.78–7.72 (m, 2H), 7.15 (br. s, 1H), 6.83 (s, 2H), 6.70 (d, $J = 9.6$ Hz, 1H), 3.45 (br. s, 2H), 3.09–2.61 (m, 6H), 1.85–1.70 (m, 4H). m/z (ES + APCI)⁺: 325 [M + H]⁺. (c) Following the procedure for **25c** using 3-(2-aminopyrimidin-5-yl)-*N*-

[2-(pyrrolidin-1-yl)ethyl]imidazo[1,2-*b*]pyridazin-6-amine, we obtained **29** as a pale yellow solid (60% yield). ¹H NMR (400 MHz, DMSO-*d*₆) δ ppm 9.97 (s, 1H), 9.17 (s, 2H), 8.24 (td, *J* = 1.4, 5.0 Hz, 1H), 7.89 (s, 1H), 7.77–7.70 (m, 2H), 7.32–7.27 (m, 1H), 7.10 (t, *J* = 5.5 Hz, 1H), 6.76 (d, *J* = 9.6 Hz, 1H), 3.41–3.33 (m, 2H), 2.67 (t, *J* = 6.9 Hz, 2H), 2.48–2.45 (m, 4H), 1.70–1.63 (m, 4H). *m/z* (ES + APCI)⁺: 420 [M + H]⁺.

3-(2-(3-Fluoropyridin-2-ylamino)pyrimidin-5-yl)-N-(4-morpholino-*trans*-cyclohexyl)imidazo[1,2-*b*]pyridazin-6-amine 30. (a) To a stirred solution of *trans*-N-(3-bromo-imidazo[1,2-*b*]pyridazin-6-yl)-cyclohexane-1,4-diamine (1.00 g, 3.24 mmol, 1.0 equiv) in *n*-BuOH (15 mL) was added K₂CO₃ (2.20 g, 15.94 mmol, 5.0 equiv) and potassium iodide (1.18 g, 7.11 mmol, 2.2 equiv) at 0 °C. After 15 min, 1-chloro-2-(2-chloroethoxy)ethane (925 mg, 6.47 mmol, 2.0 equiv) was added, and the reaction mixture was heated at 100 °C for 16 h. The reaction mixture was cooled to rt and filtered. The filtrate was diluted with dichloromethane (50 mL) and washed with H₂O (2 × 20 mL) and a brine solution (20 mL). The organic layer was dried (Na₂SO₄) and concentrated, and purification by silica gel chromatography (5% MeOH/CHCl₃) gave 3-bromo-*N*-(4-morpholino-*trans*-cyclohexyl)imidazo[1,2-*b*]pyridazin-6-amine as a yellow solid (600 mg, 49%). ¹H NMR (400 MHz, CDCl₃) δ ppm 7.58 (d, *J* = 10.0 Hz, 1H), 7.47 (s, 1H), 6.40 (d, *J* = 9.6 Hz, 1H), 4.27 (d, *J* = 6.8 Hz, 1H), 3.75–3.69 (m, 5H), 2.60–2.55 (m, 4H), 2.40–2.20 (m, 3H), 2.05–2.01 (m, 2H), 1.45–1.40 (m, 2H), 1.15–1.10 (m, 2H). *m/z* (ES)⁺: 381 [M + H]⁺. (b) Following the method for **5** using 3-bromo-*N*-(4-morpholino-*trans*-cyclohexyl)imidazo[1,2-*b*]pyridazin-6-amine (1.30 g, 3.42 mmol, 1.0 equiv), we obtained 3-(2-aminopyridin-5-yl)-*N*-(4-morpholino-*trans*-cyclohexyl)imidazo[1,2-*b*]pyridazin-6-amine as an off-white solid (950 mg, 70%). ¹H NMR (400 MHz, DMSO-*d*₆) δ ppm 8.98 (s, 2H), 7.79 (s, 1H), 7.70 (d, *J* = 10.0 Hz, 1H), 6.97 (d, *J* = 6.8 Hz, 1H), 6.86 (s, 2H), 6.62 (d, *J* = 10.0 Hz, 1H), 3.57–3.49 (m, 4H), 2.50–2.40 (m, 4H), 2.30–2.10 (m, 4H), 2.00–1.90 (m, 2H), 1.40–1.20 (m, 4H). *m/z* (APCI)⁺: 395 [M + H]⁺. (c) A mixture of 3-(2-aminopyridin-5-yl)-*N*-(4-morpholino-*trans*-cyclohexyl)imidazo[1,2-*b*]pyridazin-6-amine (150 mg, 0.38 mmol, 1.0 equiv), 2-chloro-3-fluoropyridine (100 mg, 0.76 mmol, 2.0 equiv), Xantphos (22 mg, 0.04 mmol, 0.1 equiv), and Cs₂CO₃ (496 mg, 1.52 mmol, 4.0 equiv) in 1,4-dioxane (8 mL) was degassed using argon for 45 min. Pd(PPh₃)₄ (44 mg, 0.04 mmol, 0.1 equiv) was added and the mixture further degassed for 45 min. The reaction mixture was heated at 130 °C in a sealed tube for 6 h then cooled to rt, H₂O was added (30 mL) and extracted with 20% MeOH/CHCl₃ (2 × 20 mL). The combined organic extracts were washed with brine solution (20 mL), dried (Na₂SO₄), and concentrated. The crude compound was purified by neutral alumina chromatography (2% MeOH/CHCl₃) to give **30** as a pale yellow solid (120 mg, 64%). ¹H NMR (400 MHz, DMSO-*d*₆) δ ppm 10.02 (s, 1H), 9.16 (s, 2H), 8.22 (d, *J* = 4.4 Hz, 1H), 7.88 (s, 1H), 7.73–7.67 (m, 2H), 7.31–7.27 (m, 1H), 7.06–7.04 (m, 1H), 6.66 (d, *J* = 10.0 Hz, 1H), 3.72–3.40 (m, 5H), 2.50–2.40 (m, 4H), 2.30–2.10 (m, 3H), 2.01–1.80 (m, 2H), 1.40–1.20 (m, 4H). *m/z* (ES)⁺: 490 [M + H]⁺.

3-(2-(3-Fluoropyridin-2-ylamino)pyrimidin-5-yl)-N-(4-(pyrrolidin-1-yl)-*trans*-cyclohexyl)imidazo[1,2-*b*]pyridazin-6-amine 31. (a) To a solution of **3** (500 mg, 1.61 mmol 1.0 equiv) and 1,4-dibromobutane (291 μL, 524 mg, 1.5 equiv) in anhydrous DMF (4 mL) was added K₂CO₃ (670 mg, 4.85 mmol, 3.0 equiv), and the reaction mixture was heated at 70 °C for 4 h. The reaction mixture was cooled to rt and concentrated, and purification by neutral alumina chromatography (10% MeOH/CHCl₃) gave 3-bromo-*N*-(4-(pyrrolidin-1-yl)-*trans*-cyclohexyl)imidazo[1,2-*b*]pyridazin-6-amine as an off-white solid (150 mg, 25%). ¹H NMR (400 MHz, CDCl₃) δ ppm 7.58 (d, *J* = 9.6 Hz, 1H), 7.47 (s, 1H), 6.41 (d, *J* = 10.0 Hz, 1H), 4.29 (d, *J* = 6.8 Hz, 1H), 3.77–3.71 (m, 1H), 2.62 (s, 4H), 2.27–2.24 (m, 2H), 2.12–2.08 (m, 3H), 1.8 (s, 4H), 1.52–1.46 (m, 2H), 1.29–1.23 (m, 2H). *m/z* (APCI)⁺: 364 [M + H]⁺. (b) A mixture of 3-bromo-*N*-(4-(pyrrolidin-1-yl)-*trans*-cyclohexyl)imidazo[1,2-*b*]pyridazin-6-amine (150 mg, 0.41 mmol, 1.0 equiv), 2-aminopyrimidine-5-boronic acid pinacol ester (136 mg, 0.61 mmol, 1.5 equiv), Na₂CO₃ (175 mg, 1.65 mmol, 4.0 equiv) in DMF (5 mL), and water (1 mL) was degassed using argon for 30 min. (Aphos)₂PdCl₂ (30 mg, 5 mol %) was added,

and the reaction mixture was heated at 100 °C for 4 h. The mixture was cooled to rt, concentrated, and purified by neutral alumina chromatography (10–40% MeOH/CHCl₃) to give 3-(2-aminopyrimidin-5-yl)-*N*-(4-(pyrrolidin-1-yl)-*trans*-cyclohexyl)imidazo[1,2-*b*]pyridazin-6-amine as an off-white solid (100 mg, 64%). ¹H NMR (400 MHz, DMSO-*d*₆) δ ppm 8.99 (s, 2H), 7.80 (s, 1H), 6.99 (d, *J* = 3.2 Hz, 1H), 6.86 (s, 2H), 6.71 (s, 1H), 6.62 (d, *J* = 9.6 Hz, 1H), 3.54 (s, 1H), 2.11–2.01 (m, 5H), 1.67 (s, 4H), 1.33–1.23 (m, 4H), 1.06 (s, 4H). *m/z* (APCI)⁺: 379 [M + H]⁺. (c) A mixture of 3-(2-aminopyrimidin-5-yl)-*N*-(4-(pyrrolidin-1-yl)-*trans*-cyclohexyl)imidazo[1,2-*b*]pyridazin-6-amine (100 mg, 0.26 mmol, 1.0 equiv), 2-chloro-3-fluoropyridine (52 μL, 69 mg, 0.52 mmol, 2.0 equiv), Xantphos (15 mg, 0.02 mmol, 0.1 equiv), and Cs₂CO₃ (338 mg, 1.04 mmol, 4.0 equiv) in 1,4-dioxane (5 mL) was degassed using argon for 30 min. Pd(PPh₃)₄ (30 mg, 0.02 mmol, 0.1 equiv) was then added and the mixture further degassed for 15 min. The reaction mixture was heated at 130 °C in a sealed tube for 6 h, then cooled to rt, concentrated, and purified by prep-HPLC to give **31** as an off-white solid (50 mg, 40%). ¹H NMR (400 MHz, CDCl₃) δ ppm 12.45 (s, 1H), 9.14 (s, 2H), 8.29 (d, *J* = 5.2 Hz, 1H), 7.77–7.70 (m, 2H), 7.49–7.46 (m, 1H), 7.08–7.03 (m, 1H), 6.48 (d, *J* = 10.4 Hz, 1H), 4.40 (d, *J* = 6.8 Hz, 1H), 3.72 (m, 2H), 3.08–2.91 (m, 3H), 2.42–2.26 (m, 6H), 2.01–1.85 (m, 4H), 1.43–1.31 (m, 3H). *m/z* (ES)⁺: 474 [M + H]⁺.

***N*-(3-Fluoropyridin-2-yl)-5-{6-[(1-methylpiperidin-4-yl)oxy]imidazo[1,2-*b*]pyridazin-3-yl}pyrimidin-2-amine 32.** (a) To a solution of 1-methylpiperidin-4-ol (375 mg, 3.2 mmol, 1.5 equiv) in anhydrous THF (15 mL) was added NaH (60% in mineral oil, 130 mg, 3.2 mmol, 1.5 equiv) at 0 °C. The mixture was allowed to stir at rt for 30 min, then 3-bromo-6-chloro-imidazo[1,2-*b*]pyridazine (500 mg, 2.14 mmol, 1.0 equiv) was added and heated to 65 °C for 4 h. The mixture was allowed to cool, diluted with EtOAc (100 mL), and washed with water (50 mL). The organic layer was dried (Na₂SO₄) and concentrated under reduced pressure, and purification by silica gel chromatography (5–10% MeOH/CHCl₃) gave 3-bromo-6-(1-methylpiperidin-4-yloxy)imidazo[1,2-*b*]pyridazine as a pale yellow solid (100 mg, 15%). ¹H NMR (400 MHz, DMSO-*d*₆) δ ppm 8.04 (d, *J* = 10.0 Hz, 1H), 7.74 (s, 1H), 6.93 (d, *J* = 9.6 Hz, 1H), 5.04–5.00 (m, 1H), 2.75–2.65 (m, 2H), 2.32–2.24 (m, 5H), 2.15–2.05 (m, 2H), 1.85–1.75 (m, 2H). *m/z* (APCI)⁺: 311/313 [M + H]⁺. (b) Following the method for **5** using 3-bromo-6-(1-methylpiperidin-4-yloxy)imidazo[1,2-*b*]pyridazine, we obtained 5-(6-(1-methylpiperidin-4-yloxy)imidazo[1,2-*b*]pyridazin-3-yl)pyrimidin-2-amine as a pale yellow solid (44% yield). ¹H NMR (400 MHz, DMSO-*d*₆) δ ppm 8.93 (s, 2H), 8.06–8.01 (m, 2H), 6.99 (s, 2H), 6.86 (d, *J* = 9.6 Hz, 1H), 4.95–4.85 (m, 1H), 2.75–2.65 (m, 2H), 2.19–2.08 (m, 7H), 1.79–1.74 (m, 2H). *m/z* (APCI)⁺: 326 [M + H]⁺. (c) Following the method for **30c** using 5-(6-(1-methylpiperidin-4-yloxy)imidazo[1,2-*b*]pyridazin-3-yl)pyrimidin-2-amine, we obtained **32** as a pale yellow solid (42% yield). ¹H NMR (400 MHz, CDCl₃) δ ppm 9.16 (s, 2H), 8.30 (d, *J* = 4.4 Hz, 1H), 7.87 (d, *J* = 8.2 Hz, 2H), 7.72 (s, 1H), 7.49–7.44 (m, 1H), 7.08–7.04 (m, 1H), 6.75 (d, *J* = 10.0 Hz, 1H), 5.10–5.00 (m, 1H), 2.70–2.65 (m, 2H), 2.45–2.35 (m, 2H), 2.33 (s, 3H), 2.13–2.10 (m, 2H), 1.94–1.92 (m, 2H). *m/z* (APCI)⁺: 421 [M + H]⁺.

(*R,S*)-*N*-(3-Fluoropyridin-2-yl)-5-{6-[(1-methylpyrrolidin-3-yl)oxy]imidazo[1,2-*b*]pyridazin-3-yl}pyrimidin-2-amine 33. (a) Following the method for **32a** using (*R,S*)-1-methylpyrrolidin-3-ol, we obtained (*R,S*)-3-bromo-6-[(1-methylpyrrolidin-3-yl)oxy]imidazo[1,2-*b*]pyridazine as a pale yellow solid (1.4 g, crude). ¹H NMR (400 MHz, CDCl₃) δ ppm 7.74 (d, *J* = 9.6 Hz, 1H), 7.59 (s, 1H), 6.73 (d, *J* = 8.0 Hz, 1H), 5.48–5.44 (m, 1H), 2.97–2.89 (m, 2H), 2.82–2.78 (m, 1H), 2.52–2.45 (m, 1H), 2.42 (s, 3H), 2.40–2.34 (m, 1H), 2.10–2.04 (m, 1H). *m/z* (APCI)⁺: 297/299 [M + H]⁺. (b) Following the method for **5** using (*R,S*)-3-bromo-6-[(1-methylpyrrolidin-3-yl)oxy]imidazo[1,2-*b*]pyridazine, we obtained (*R,S*)-5-(6-(1-methylpyrrolidin-3-yloxy)imidazo[1,2-*b*]pyridazin-3-yl)pyrimidin-2-amine as a pale yellow solid (39%). ¹H NMR (400 MHz, CDCl₃) δ ppm 8.93 (s, 2H), 7.84 (d, *J* = 9.2 Hz, 1H), 7.81 (s, 1H), 6.75 (d, *J* = 8.0 Hz, 1H), 5.40–5.35 (m, 1H), 5.22 (br. s, 2H), 3.05–2.97 (m, 2H), 2.70–2.65 (m, 1H), 2.42 (s, 3H), 2.35–2.30 (m, 1H), 2.11–2.03 (m, 2H). *m/z* (APCI)⁺: 312 [M + H]⁺. (c) Following the method for **30c** using

(R,S)-5-(6-(1-methylpyrrolidin-3-yloxy)imidazo[1,2-*b*]pyridazin-3-yl)-pyrimidin-2-amine, we obtained **33** as a pale yellow solid (90 mg, 53%). ¹H NMR (400 MHz, CDCl₃) δ ppm 9.18 (s, 2H), 8.30 (d, *J* = 4.4 Hz, 1H), 7.88 (s, 1H), 7.86 (d, *J* = 9.6 Hz, 1H), 7.74 (s, 1H), 7.47 (t, *J* = 8.0 Hz, 1H), 7.07 (m, 1H), 6.78 (d, *J* = 8.0 Hz, 1H), 5.45–5.40 (m, 1H), 3.04–2.94 (m, 2H), 2.70–2.65 (m, 1H), 2.51–2.43 (m, 1H), 2.41 (s, 3H), 2.36–2.27 (m, 1H), 2.11–2.04 (m, 1H). *m/z* (APCI)⁺: 325 [M + H]⁺.

N-(3-Fluoropyridin-2-yl)-5-[6-[(1-methylpiperidin-4-yl)methyl]imidazo[1,2-*b*]pyridazin-3-yl]pyrimidin-2-amine **34**. (a) To a solution of 1-Boc-4-methylene-piperidine (1.29 g, 6.5 mmol, 2.0 equiv) in dry THF (10 mL) under nitrogen was added 9-BBN (0.5 M in THF, 16.3 mL, 8.16 mmol, 2.5 equiv). The reaction mixture was heated at 75 °C for 3 h. After cooling, the resulting solution was added to a mixture of 6-chloroimidazo[1,2-*b*]pyridazine (0.5 g, 3.2 mmol), Pd(dppf)Cl₂ (133 mg, 0.16 mmol, 0.05 equiv), and K₂CO₃ (1.35 g, 9.8 mmol, 3.0 equiv) in DMF (5 mL) and water (1 mL). The reaction mixture was heated at 75 °C for 16 h then concentrated under reduced pressure. The residue was dissolved in EtOAc and washed with water (50 mL) and brine (20 mL). The organics were dried over MgSO₄ and concentrated under reduced pressure. Purification by chromatography on silica gel gave *tert*-butyl 4-(imidazo[1,2-*b*]pyridazin-6-ylmethyl)piperidine-1-carboxylate as a solid (0.406 g, 40%). ¹H NMR (400 MHz, DMSO-*d*₆) δ ppm 8.21 (s, 1H), 8.03 (d, *J* = 9.1 Hz, 1H), 7.71 (s, 1H), 7.16 (d, *J* = 9.1 Hz, 1H), 3.91 (m, 2H), 2.79–2.55 (m, 4H), 1.92 (m, 1H), 1.65–1.52 (m, 2H), 1.38 (s, 9H), 1.22–0.99 (m, 2H). *m/z* (ES + APCI)⁺: 317 [M + H]⁺. (b) To a solution of *tert*-butyl 4-(imidazo[1,2-*b*]pyridazin-6-ylmethyl)piperidine-1-carboxylate (0.40 g, 1.26 mmol) in dry CH₂Cl₂ (6 mL) was added dropwise a solution of NBS (0.246 g, 1.39 mmol, 1.1 equiv) in dry acetonitrile (6 mL). The reaction mixture was stirred at room temperature for 1 h. NBS (24 mg, 0.13 mmol) was added, and the reaction mixture was stirred for a further hour. The reaction mixture was concentrated under reduced pressure. The residue was dissolved in CH₂Cl₂ (100 mL) and washed with water (2 × 30 mL). The organics were dried over MgSO₄ and concentrated under reduced pressure. Purification by chromatography on silica gel gave *tert*-butyl 4-[(3-bromoimidazo[1,2-*b*]pyridazin-6-yl)methyl]piperidine-1-carboxylate as a solid (0.42 g, 83%). ¹H NMR (400 MHz, DMSO-*d*₆) δ ppm 8.09 (d, *J* = 9.1 Hz, 1H), 7.86 (s, 1H), 7.26 (d, *J* = 9.1 Hz, 1H), 3.96–3.82 (m, 2H), 2.80 (d, *J* = 6.9 Hz, 2H), 2.77–2.59 (m, 2H), 1.98–1.87 (m, 1H), 1.64–1.55 (m, 2H), 1.38 (s, 9H), 1.24–1.01 (m, 2H). (c) Following the method for **5**, we obtained *tert*-butyl 4-[(3-(2-aminopyrimidin-5-yl)imidazo[1,2-*b*]pyridazin-6-yl)methyl]piperidine-1-carboxylate as a yellow solid (0.170 g, 70%). ¹H NMR (400 MHz, DMSO-*d*₆) δ ppm 8.93 (s, 2H), 8.10 (s, 1H), 8.09 (d, *J* = 9.1 Hz, 1H), 7.18 (d, *J* = 9.1 Hz, 1H), 6.93 (br. s, 2H), 3.95–3.85 (m, 2H), 2.79 (d, *J* = 7.3 Hz, 2H), 2.75–2.55 (m, 2H), 2.03–1.89 (m, 1H), 1.70–1.58 (m, 2H), 1.38 (s, 9H), 1.21–1.03 (m, 2H). *m/z* (ES + APCI)⁺: 410 [M + H]⁺. (d) Following the method for **25c**, we obtained *tert*-butyl 4-[(3-{2-[(3-fluoropyridin-2-yl)amino]pyrimidin-5-yl}imidazo[1,2-*b*]pyridazin-6-yl)methyl]piperidine-1-carboxylate as a yellow solid (0.10 g, 48%). ¹H NMR (400 MHz, CD₃OD) δ ppm 9.21 (s, 2H), 8.24–8.20 (m, 1H), 8.12 (s, 1H), 8.01 (d, *J* = 9.6 Hz, 1H), 7.67 (ddd, *J* = 10.2, 8.4, 1.6 Hz, 1H), 7.31–7.18 (m, 2H), 4.13–4.01 (m, 2H), 2.87 (d, *J* = 7.3 Hz, 2H), 2.85–2.65 (m, 2H), 2.15–2.05 (m, 1H), 1.80–1.65 (m, 2H), 1.44 (s, 9H), 1.32–1.15 (m, 2H). *m/z* (ES + APCI)⁺: 505 [M + H]⁺. (e) To a solution of *tert*-butyl 4-[(3-{2-[(3-fluoropyridin-2-yl)amino]pyrimidin-5-yl}imidazo[1,2-*b*]pyridazin-6-yl)methyl]piperidine-1-carboxylate (0.10 g, 0.19 mmol) in MeOH (2 mL) was added 4 M HCl (2 mL), and the reaction mixture was stirred at room temperature for 2 h. The reaction mixture was concentrated under reduced pressure. The residue was purified by prep-LCMS to give the product as a TFA salt, which was eluted through an Isolute aminopropyl cartridge to give *N*-(3-fluoropyridin-2-yl)-5-[6-(piperidin-4-ylmethyl)imidazo[1,2-*b*]pyridazin-3-yl]pyrimidin-2-amine as a solid (75 mg, 94%). ¹H NMR (400 MHz, CD₃OD) δ ppm 9.20 (s, 2H), 8.24–8.19 (m, 1H), 8.12 (s, 1H), 8.01 (d, *J* = 9.1 Hz, 1H), 7.67 (ddd, *J* = 10.5, 8.2, 1.3 Hz, 1H), 7.31–7.21 (m, 2H), 3.13–3.04 (m, 2H), 2.88 (d, *J* = 7.3 Hz, 2H), 2.67 (td, *J* = 12.5, 2.7 Hz, 2H), 2.30–2.07 (m, 1H), 1.77 (m, 2H), 1.34 (qd, *J* = 12.5, 4.1 Hz, 2H). *m/z* (ES

+ APCI)⁺: 405 [M + H]⁺. (f) Following the procedure for **19b**, we obtained **34** as a yellow solid (34 mg, 65%). ¹H NMR (400 MHz, CD₃OD) δ ppm 9.16 (s, 2H), 8.25–8.17 (m, 1H), 8.10 (s, 1H), 8.01 (d, *J* = 9.1 Hz, 1H), 7.66 (ddd, *J* = 10.1, 8.2, 1.0 Hz, 1H), 7.30–7.21 (m, 2H), 3.48 (m, 2H), 3.09–2.97 (m, 2H), 2.94 (d, *J* = 6.8 Hz, 2H), 2.84 (s, 3H), 2.31–2.13 (m, 1H), 2.02 (m, 2H), 1.71–1.53 (m, 2H). *m/z* (ES + APCI)⁺: 419 [M + H]⁺.

3-[4-[(3-Fluoropyridin-2-yl)amino]phenyl]-*N*-(1-methylpiperidin-4-yl)imidazo[1,2-*b*]pyridazin-6-amine **35**. (a) Following the method for **5** using **17** and 4-aminophenylboronic acid pinacol ester, we obtained *tert*-butyl 4-[[3-(4-aminophenyl)imidazo[1,2-*b*]pyridazin-6-yl]amino]piperidine-1-carboxylate as a yellow solid (84% yield). ¹H NMR (400 MHz, DMSO-*d*₆) δ ppm 7.88–7.78 (m, 2H), 7.68 (d, *J* = 9.6 Hz, 1H), 7.63 (s, 1H), 6.94 (d, *J* = 6.4 Hz, 1H), 6.67–6.60 (m, 2H), 6.58 (d, *J* = 9.6 Hz, 1H), 5.27 (s, 2H), 4.01–3.85 (m, 2H), 3.85–3.70 (m, 1H), 3.05–2.87 (m, 2H), 2.13–2.00 (m, 2H), 1.48–1.27 (m, 11H). *m/z* (ES + APCI)⁺: 409 [M + H]⁺. (b) Following the method for **7** using *tert*-butyl 4-[[3-(4-aminophenyl)imidazo[1,2-*b*]pyridazin-6-yl]amino]piperidine-1-carboxylate, we obtained 3-[4-[(3-fluoropyridin-2-yl)amino]phenyl]-*N*-(piperidin-4-yl)imidazo[1,2-*b*]pyridazin-6-amine as an off-white solid (25% yield). ¹H NMR (400 MHz, DMSO-*d*₆) δ ppm 8.97 (d, *J* = 1.8 Hz, 1H), 8.15–8.06 (m, *J* = 8.7 Hz, 2H), 8.05–7.98 (m, 1H), 7.92–7.84 (m, *J* = 8.7 Hz, 2H), 7.80 (s, 1H), 7.72 (d, *J* = 9.6 Hz, 1H), 7.57 (ddd, *J* = 1.4, 9.7, 11.8 Hz, 1H), 6.96 (d, *J* = 6.9 Hz, 1H), 6.83 (ddd, *J* = 3.2, 4.8, 8.0 Hz, 1H), 6.65 (d, *J* = 9.6 Hz, 1H), 3.79–3.62 (m, 1H), 3.09–2.96 (m, 2H), 2.66–2.56 (m, 2H), 2.12–1.98 (m, 2H), 1.44–1.25 (m, 2H). *m/z* (ES + APCI)⁺: 404 [M + H]⁺. (c) Following the method for **19b** using 3-[4-[(3-fluoropyridin-2-yl)amino]phenyl]-*N*-(piperidin-4-yl)imidazo[1,2-*b*]pyridazin-6-amine, we obtained **35** as a yellow solid (70% yield). ¹H NMR (400 MHz, DMSO-*d*₆) δ ppm 9.00 (d, *J* = 1.8 Hz, 1H), 8.14–8.06 (m, 2H), 8.04–7.97 (m, 1H), 7.94–7.85 (m, 2H), 7.80 (s, 1H), 7.72 (d, *J* = 9.6 Hz, 1H), 7.62–7.51 (m, 1H), 6.97 (d, *J* = 6.4 Hz, 1H), 6.84 (ddd, *J* = 3.4, 4.7, 7.9 Hz, 1H), 6.65 (d, *J* = 9.6 Hz, 1H), 3.68–3.47 (m, 1H), 2.89–2.74 (m, 2H), 2.20 (s, 3H), 2.12–1.99 (m, 4H), 1.60–1.42 (m, 2H). *m/z* (ES + APCI)⁺: 418 [M + H]⁺.

3-[3-Fluoro-4-(pyridin-2-ylamino)phenyl]-*N*-(1-methylpiperidin-4-yl)imidazo[1,2-*b*]pyridazin-6-amine **36**. (a) Following the method for **5** using **17** and 4-amino-3-fluorophenylboronic acid pinacol ester, we obtained *tert*-butyl 4-[[3-(4-amino-3-fluorophenyl)imidazo[1,2-*b*]pyridazin-6-yl]amino]piperidine-1-carboxylate as an off-white solid (56% yield). ¹H NMR (400 MHz, DMSO-*d*₆) δ ppm 7.98 (dd, *J* = 2.1, 14.0 Hz, 1H), 7.78 (s, 1H), 7.73 (d, *J* = 9.6 Hz, 1H), 7.64 (dd, *J* = 1.8, 8.2 Hz, 1H), 7.08 (d, *J* = 6.4 Hz, 1H), 6.83 (dd, *J* = 8.2, 9.6 Hz, 1H), 6.64 (d, *J* = 9.6 Hz, 1H), 5.35 (br. s, 2H), 4.04–3.88 (m, 2H), 3.84–3.69 (m, 1H), 3.05–2.85 (m, 2H), 2.14–2.04 (m, 2H), 1.45–1.28 (m, 11H). *m/z* (ES + APCI)⁺: 427 [M + H]⁺. (b) Following the method for **7** using *tert*-butyl 4-[[3-(4-amino-3-fluorophenyl)imidazo[1,2-*b*]pyridazin-6-yl]amino]piperidine-1-carboxylate and 2-chloropyridine, we obtained 3-[3-fluoro-4-(pyridin-2-ylamino)phenyl]-*N*-(piperidin-4-yl)imidazo[1,2-*b*]pyridazin-6-amine as a yellow solid (28% yield). ¹H NMR (400 MHz, DMSO-*d*₆) δ ppm 8.89–8.75 (m, 1H), 8.36–8.25 (m, 2H), 8.16 (dd, *J* = 1.4, 5.0 Hz, 1H), 7.90 (s, 1H), 7.84 (dd, *J* = 1.8, 8.7 Hz, 1H), 7.74 (d, *J* = 10.1 Hz, 1H), 7.59 (ddd, *J* = 1.8, 7.0, 8.6 Hz, 1H), 7.08–6.98 (m, 2H), 6.79 (ddd, *J* = 0.9, 5.5, 6.4 Hz, 1H), 6.67 (d, *J* = 9.6 Hz, 1H), 3.77–3.62 (m, 1H), 3.08–2.94 (m, 2H), 2.65–2.54 (m, 2H), 2.16–1.97 (m, 2H), 1.42–1.25 (m, 2H). *m/z* (ES + APCI)⁺: 404 [M + H]⁺. (c) Following the method for **19b** using 3-[3-fluoro-4-(pyridin-2-ylamino)phenyl]-*N*-(piperidin-4-yl)imidazo[1,2-*b*]pyridazin-6-amine, we obtained **36** as a yellow solid (62% yield). ¹H NMR (400 MHz, DMSO-*d*₆) δ ppm 8.84 (s, 1H), 8.39–8.27 (m, 2H), 8.16 (td, *J* = 1.4, 5.0 Hz, 1H), 7.91 (s, 1H), 7.82 (dd, *J* = 1.8, 8.7 Hz, 1H), 7.75 (d, *J* = 9.6 Hz, 1H), 7.63–7.54 (m, 1H), 7.11–6.99 (m, 2H), 6.79 (ddd, *J* = 0.9, 5.5, 6.4 Hz, 1H), 6.68 (d, *J* = 9.6 Hz, 1H), 3.70–3.51 (m, 1H), 2.89–2.75 (m, 2H), 2.19 (s, 3H), 2.16–1.99 (m, 4H), 1.60–1.40 (m, 2H). *m/z* (ES + APCI)⁺: 418 [M + H]⁺.

3-[3,5-Difluoro-4-(pyridin-2-ylamino)phenyl]-*N*-(1-methylpiperidin-4-yl)imidazo[1,2-*b*]pyridazin-6-amine **37**. (a) A solution of 4-bromo-2,6-difluoroaniline (2.50 g, 12.0 mmol, 1.0 equiv), bis-(pinacolato)diboron (3.36 g, 13.2 mmol, 1.1 equiv), Pd(dppf)Cl₂

(150 mg, 0.18 mmol, 15 mol %), and potassium acetate (3.54 g, 36.06 mmol, 3.0 equiv) in DMSO was heated at 80 °C under N₂ for 90 min. The reaction mixture was partitioned between EtOAc (100 mL) and saturated aqueous bicarbonate (100 mL). The organic layer was washed with brine (3 × 100 mL), dried over MgSO₄, and concentrated under reduced pressure to give 2,6-difluoro-4-(4,4,5,5-tetramethyl-1,3,2-dioxaborolan-2-yl)aniline as a brown solid (3.0 g, 97%). ¹H NMR (400 MHz, DMSO-*d*₆) δ ppm 7.07–6.94 (m, 2H), 5.66 (s, 2H), 1.28–1.17 (m, 12H). *m/z* (ES + APCI)⁺: 256 [M + H]⁺. (b) To a solution of 1-methylpiperidine-4-amine (11.8 g, 103 mmol, 3.0 equiv) in NMP (32 mL) was added 3-bromo-6-chloroimidazo[1,2-*b*]pyridazine (8.0 g, 34.0 mmol, 1.0 equiv). The reaction mixture was heated in a microwave at 180 °C for 35 min. The reaction mixture was diluted with ethyl acetate (200 mL) and washed with deionized water (3 × 250 mL). The organic layer was separated, dried (MgSO₄), filtered, and concentrated under reduced pressure. Purification by chromatography on silica gel (2.5%–25% 2 M NH₃ in MeOH/EtOAc) gave 3-bromo-*N*-(1-methylpiperidin-4-yl)imidazo[1,2-*b*]pyridazin-6-amine as a pale yellow solid (4.8 g, 45%). ¹H NMR (400 MHz, CD₃OD) δ ppm 7.52 (d, *J* = 9.6 Hz, 1H), 7.37 (s, 1H), 6.67 (d, *J* = 9.6 Hz, 1H), 3.91–3.66 (m, 1H), 2.97–2.78 (m, 2H), 2.30 (s, 3H), 2.26–2.08 (m, 4H), 1.79–1.72 (m, 2H). *m/z* (ES + APCI)⁺: 310 [M + H]⁺. (c) Following the method for 5 using 3-bromo-*N*-(1-methylpiperidin-4-yl)imidazo[1,2-*b*]pyridazin-6-amine and 2,6-difluoro-4-(4,4,5,5-tetramethyl-1,3,2-dioxaborolan-2-yl)aniline, we obtained 3-(4-amino-3,5-difluorophenyl)-*N*-(1-methylpiperidin-4-yl)imidazo[1,2-*b*]pyridazin-6-amine as a yellow solid (521 mg, 45%). ¹H NMR (400 MHz, DMSO-*d*₆) δ ppm 7.96–7.80 (m, 3H), 7.71 (d, *J* = 9.6 Hz, 1H), 7.05 (d, *J* = 6.9 Hz, 1H), 6.64 (d, *J* = 9.6 Hz, 1H), 5.40 (s, 2H), 3.67–3.42 (m, 1H), 2.91–2.76 (m, 2H), 2.19 (s, 3H), 2.15–1.94 (m, 4H), 1.59–1.34 (m, 2H). *m/z* (ES + APCI)⁺: 359 [M + H]⁺. (d) Following the method for 25c using 3-(4-amino-3,5-difluorophenyl)-*N*-(1-methylpiperidin-4-yl)imidazo[1,2-*b*]pyridazin-6-amine and 2-chloropyridine, we obtained 37 as a yellow solid (9% yield). ¹H NMR (400 MHz, DMSO-*d*₆) δ ppm 8.54 (s, 1H), 8.07–8.00 (m, 3H), 7.98 (dd, *J* = 1.4, 5.0 Hz, 1H), 7.75 (d, *J* = 9.6 Hz, 1H), 7.52 (ddd, *J* = 1.8, 7.0, 8.6 Hz, 1H), 7.13 (d, *J* = 6.4 Hz, 1H), 6.77–6.60 (m, 3H), 3.67–3.43 (m, 1H), 2.93–2.69 (m, 2H), 2.16 (br. s, 3H), 2.12–1.92 (m, 4H), 1.61–1.32 (m, 2H). *m/z* (ES + APCI)⁺: 436 [M + H]⁺.

3-[6-[(3-Fluoropyridin-2-yl)amino]pyridin-3-yl]-*N*-[*trans*-4-(pyrrolidin-1-yl)cyclohexyl]imidazo[1,2-*b*]pyridazin-6-amine 38. (a) Following the procedure for 5 using 3-bromo-*N*-4-(pyrrolidin-1-yl)-*trans*-cyclohexylimidazo[1,2-*b*]pyridazin-6-amine (500 mg, 1.37 mmol, 1.0 equiv) and 2-aminopyridine-5-boronic acid pinacol ester (452 mg, 2.06 mmol, 1.5 equiv), we obtained 3-(6-aminopyridin-3-yl)-*N*-[*trans*-4-(pyrrolidin-1-yl)cyclohexyl]imidazo[1,2-*b*]pyridazin-6-amine as a beige solid (468 mg, 90%). ¹H NMR (400 MHz, DMSO-*d*₆) δ ppm 8.76–8.73 (m, 1H), 8.08 (dd, *J* = 2.3, 8.7 Hz, 1H), 7.70–7.66 (m, 2H), 6.93 (d, *J* = 6.9 Hz, 1H), 6.59 (d, *J* = 9.6 Hz, 1H), 6.53 (d, *J* = 8.7 Hz, 1H), 6.11 (s, 2H), 3.64–3.46 (m, 1H), 2.88–2.61 (m, 3H), 2.21–2.00 (m, 5H), 1.84–1.63 (m, 4H), 1.44–1.19 (m, 5H). *m/z* (ES + APCI)⁺: 378 [M + H]⁺. (b) Following the method for 25c using 3-(6-aminopyridin-3-yl)-*N*-[*trans*-4-(pyrrolidin-1-yl)cyclohexyl]imidazo[1,2-*b*]pyridazin-6-amine, we obtained 38 as a pale yellow solid (24% yield). ¹H NMR (400 MHz, DMSO-*d*₆) δ ppm 9.37–9.32 (m, 1H), 9.11 (d, *J* = 1.8 Hz, 1H), 8.42 (dd, *J* = 2.3, 8.7 Hz, 1H), 8.11–8.06 (m, 2H), 7.88 (s, 1H), 7.73 (d, *J* = 9.6 Hz, 1H), 7.67–7.61 (m, 1H), 7.04–6.96 (m, 2H), 6.66 (d, *J* = 9.6 Hz, 1H), 3.58 (br. s, 1H), 2.74–2.51 (m, 3H), 2.19–2.08 (m, *J* = 8.7 Hz, 2H), 2.07–1.96 (m, 3H), 1.72–1.63 (m, 4H), 1.37–1.20 (m, 5H). *m/z* (ES + APCI)⁺: 473 [M + H]⁺.

3-[4-[(3-Fluoropyridin-2-yl)amino]phenyl]-*N*-[*trans*-4-(pyrrolidin-1-yl)cyclohexyl]imidazo[1,2-*b*]pyridazin-6-amine 39. (a) Following the method for 5 using 3-bromo-*N*-[*trans*-4-(pyrrolidin-1-yl)cyclohexyl]imidazo[1,2-*b*]pyridazin-6-amine and 4-aminophenylboronic acid pinacol ester, we obtained 3-(4-aminophenyl)-*N*-[*trans*-4-(pyrrolidin-1-yl)cyclohexyl]imidazo[1,2-*b*]pyridazin-6-amine as an off-white solid (37% yield). ¹H NMR (400 MHz, DMSO-*d*₆) δ ppm 7.90–7.81 (m, 2H), 7.69–7.60 (m, 2H), 6.84 (d, *J* = 6.9 Hz, 1H), 6.67–6.59 (m, 2H), 6.59–6.50 (m, 2H), 5.27 (s, 2H), 2.61–2.52 (m, 3H), 2.23–2.09 (m, 2H), 2.09–1.94 (m, 3H), 1.74–1.62 (m, 4H),

1.36–1.13 (m, 5H). *m/z* (ES + APCI)⁺: 377 [M + H]⁺. (b) Following the method for 25c using 3-(4-aminophenyl)-*N*-[*trans*-4-(pyrrolidin-1-yl)cyclohexyl]imidazo[1,2-*b*]pyridazin-6-amine, we obtained 39 as an off-white solid (27% yield). ¹H NMR (400 MHz, DMSO-*d*₆) δ ppm 8.99 (d, *J* = 1.8 Hz, 1H), 8.18–8.06 (m, 2H), 8.00 (d, *J* = 5.0 Hz, 1H), 7.94–7.85 (m, *J* = 9.2 Hz, 2H), 7.80 (s, 1H), 7.71 (d, *J* = 9.6 Hz, 1H), 7.57 (ddd, *J* = 1.6, 8.1, 11.8 Hz, 1H), 6.94 (d, *J* = 6.9 Hz, 1H), 6.84 (ddd, *J* = 3.2, 4.8, 8.0 Hz, 1H), 6.63 (d, *J* = 9.6 Hz, 1H), 3.66–3.51 (m, 1H), 2.58–2.52 (m, 3H), 2.24–2.11 (m, 2H), 2.10–1.95 (m, 3H), 1.74–1.61 (m, 4H), 1.40–1.20 (m, 5H). *m/z* (ES + APCI)⁺: 472 [M + H]⁺.

trans-*N*-(3-[4-[(3-Fluoropyridin-2-yl)amino]phenyl]imidazo[1,2-*b*]pyridazin-6-yl)cyclohexane-1,4-diamine 40. (a) Following the method for 5 using 4 and 4-aminophenylboronic acid pinacol ester, we obtained *tert*-butyl (*trans*-4-{[3-(4-aminophenyl)imidazo[1,2-*b*]pyridazin-6-yl]amino}cyclohexyl)carbamate as a yellow solid (66% yield). ¹H NMR (400 MHz, DMSO-*d*₆) δ ppm 7.95–7.76 (m, 2H), 7.65 (d, *J* = 9.6 Hz, 1H), 7.63–7.58 (m, 1H), 6.84 (d, *J* = 6.9 Hz, 1H), 6.79 (s, 1H), 6.70–6.59 (m, 2H), 6.56 (d, *J* = 10.1 Hz, 1H), 5.26 (s, 2H), 3.64–3.42 (m, 1H), 3.39–3.13 (m, 1H), 2.24–2.10 (m, 2H), 1.93–1.76 (m, 2H), 1.39 (s, 9H), 1.35–1.17 (m, 4H). *m/z* (ES + APCI)⁺: 423 [M + H]⁺. (b) Following the method for 7 using *tert*-butyl (*trans*-4-{[3-(4-aminophenyl)imidazo[1,2-*b*]pyridazin-6-yl]amino}cyclohexyl)carbamate, we obtained 40 as a yellow solid (17% yield). ¹H NMR (400 MHz, DMSO-*d*₆) δ ppm 9.00 (d, *J* = 1.8 Hz, 1H), 8.15–8.07 (m, 2H), 8.05–7.97 (m, 1H), 7.93–7.85 (m, 2H), 7.79 (s, 1H), 7.70 (d, *J* = 9.6 Hz, 1H), 7.57 (ddd, *J* = 1.6, 8.1, 11.8 Hz, 1H), 6.89 (d, *J* = 6.9 Hz, 1H), 6.83 (ddd, *J* = 3.2, 4.8, 8.0 Hz, 1H), 6.63 (d, *J* = 9.6 Hz, 1H), 3.61–3.46 (m, 1H), 2.69–2.55 (m, 1H), 2.19–2.09 (m, 2H), 1.90–1.79 (m, 2H), 1.34–1.10 (m, 4H). *m/z* (ES + APCI)⁺: 418 [M + H]⁺.

3-[4-[(5-Chloro-3-fluoropyridin-2-yl)amino]phenyl]-*N*-(1-methylpiperidin-4-yl)imidazo[1,2-*b*]pyridazin-6-amine 41. (a) Following the method for 5 using 3-bromo-*N*-(1-methylpiperidin-4-yl)imidazo[1,2-*b*]pyridazin-6-amine and 4-aminophenylboronic acid pinacol ester, we obtained 3-(4-aminophenyl)-*N*-(1-methylpiperidin-4-yl)imidazo[1,2-*b*]pyridazin-6-amine as a yellow solid (42% yield). ¹H NMR (400 MHz, DMSO-*d*₆) δ ppm 7.93–7.79 (m, 2H), 7.66 (d, *J* = 9.6 Hz, 1H), 7.63 (s, 1H), 6.89 (d, *J* = 6.4 Hz, 1H), 6.66–6.60 (m, 2H), 6.58 (d, *J* = 9.6 Hz, 1H), 5.28 (s, 2H), 3.70–3.47 (m, 1H), 2.88–2.77 (m, 2H), 2.21 (s, 3H), 2.11–1.93 (m, 4H), 1.59–1.35 (m, 2H). *m/z* (ES + APCI)⁺: 323 [M + H]⁺. (b) Following the method for 25c using 3-(4-aminophenyl)-*N*-(1-methylpiperidin-4-yl)imidazo[1,2-*b*]pyridazin-6-amine, we obtained 41 as a yellow solid (32% yield). ¹H NMR (400 MHz, DMSO-*d*₆) δ ppm 9.18 (d, *J* = 1.8 Hz, 1H), 8.22–8.02 (m, 3H), 7.97–7.77 (m, 4H), 7.72 (d, *J* = 9.6 Hz, 1H), 6.97 (d, *J* = 6.4 Hz, 1H), 6.65 (d, *J* = 9.6 Hz, 1H), 3.73–3.51 (m, 1H), 2.91–2.72 (m, 2H), 2.21 (s, 3H), 2.13–1.95 (m, 4H), 1.61–1.35 (m, 2H). *m/z* (ES + APCI)⁺: 452 [M + H]⁺.

3-[4-[(3-Fluoro-6-methylpyridin-2-yl)amino]phenyl]-*N*-(1-methylpiperidin-4-yl)imidazo[1,2-*b*]pyridazin-6-amine 42. Following the method for 41 using 2-bromo-3-fluoro-6-methylpyridine, we obtained 42 as a yellow solid (15% yield). ¹H NMR (400 MHz, DMSO-*d*₆) δ ppm 8.91 (d, *J* = 2.3 Hz, 1H), 8.21–8.05 (m, 2H), 8.03–7.89 (m, 2H), 7.82 (s, 1H), 7.72 (d, *J* = 9.6 Hz, 1H), 7.44 (dd, *J* = 8.0, 11.7 Hz, 1H), 6.98 (d, *J* = 6.4 Hz, 1H), 6.76–6.54 (m, 2H), 3.70–3.48 (m, 1H), 2.92–2.77 (m, 2H), 2.39 (s, 3H), 2.20 (s, 3H), 2.15–1.94 (m, 4H), 1.58–1.39 (m, 2H). *m/z* (ES + APCI)⁺: 432 [M + H]⁺.

3-[4-[(3,5-Difluoropyridin-2-yl)amino]phenyl]-*N*-(1-methylpiperidin-4-yl)imidazo[1,2-*b*]pyridazin-6-amine 43. Following the method for 41 using 2-bromo-3,5-difluoropyridine, we obtained 43 as a yellow solid (27% yield). ¹H NMR (400 MHz, DMSO-*d*₆) δ ppm 9.02 (d, *J* = 1.8 Hz, 1H), 8.15–8.04 (m, 3H), 7.89–7.78 (m, 4H), 7.72 (d, *J* = 9.6 Hz, 1H), 6.97 (d, *J* = 6.4 Hz, 1H), 6.65 (d, *J* = 9.6 Hz, 1H), 3.68–3.51 (m, 1H), 2.85–2.74 (m, 2H), 2.20 (s, 3H), 2.12–1.98 (m, 4H), 1.56–1.43 (m, 2H). *m/z* (ES + APCI)⁺: 436 [M + H]⁺.

N-(1-Methylpiperidin-4-yl)-3-[4-[(5-(trifluoromethyl)pyridin-2-yl)amino]phenyl]imidazo[1,2-*b*]pyridazin-6-amine 44. Following the method for 41 using 2-chloro-5-trifluoromethylpyridine, we obtained 44 as an off-white solid (7% yield). ¹H NMR (400 MHz, CD₃OD) δ

ppm 8.45–8.40 (m, 1H), 8.13–8.06 (m, 2H), 7.79–7.68 (m, 4H), 7.61 (d, $J = 9.6$ Hz, 1H), 6.92 (d, $J = 8.7$ Hz, 1H), 6.68 (d, $J = 9.6$ Hz, 1H), 3.84–3.74 (m, 1H), 2.99–2.90 (m, 2H), 2.36 (s, 3H), 2.33–2.16 (m, 4H), 1.72–1.57 (m, 2H). m/z (ES + APCI)⁺: 468 [M + H]⁺.

3-(4-[[3-Fluoro-6-(trifluoromethyl)pyridin-2-yl]amino]phenyl)-N-(1-methylpiperidin-4-yl)imidazo[1,2-b]pyridazin-6-amine 45. Following the procedure for **41** using 2-chloro-6-trifluoromethylpyridine, we obtained **45** as an off-white solid (12% yield). ¹H NMR (400 MHz, CD₃OD) δ ppm 8.06–8.01 (m, 2H), 7.91–7.85 (m, 2H), 7.76–7.70 (m, 2H), 7.67 (d, $J = 9.6$ Hz, 1H), 7.14 (d, $J = 7.3$ Hz, 1H), 7.03 (d, $J = 8.7$ Hz, 1H), 6.70 (d, $J = 9.6$ Hz, 1H), 4.05–3.95 (m, 1H), 3.57–3.40 (m, 2H), 3.21–3.01 (m, 2H), 2.83 (s, 3H), 2.53–2.38 (m, 2H), 1.99–1.69 (m, 2H) m/z (ES + APCI)⁺: 468 [M + H]⁺.

trans-N-(3-{4-[(3,5-Difluoropyridin-2-yl)amino]phenyl}imidazo[1,2-b]pyridazin-6-yl)cyclohexane-1,4-diamine 46. Following the method for **40** using 2-bromo-3,5-difluoropyridine, we obtained **46** as a yellow solid (31% yield). ¹H NMR (400 MHz, DMSO-*d*₆) δ ppm 9.03 (d, $J = 1.8$ Hz, 1H), 8.16–8.04 (m, 3H), 7.89–7.78 (m, 4H), 7.70 (d, $J = 9.6$ Hz, 1H), 6.90 (d, $J = 6.9$ Hz, 1H), 6.62 (d, $J = 9.6$ Hz, 1H), 3.60–3.48 (m, 1H), 2.68–2.57 (m, 1H), 2.19–2.10 (m, 2H), 1.90–1.80 (m, 2H), 1.32–1.13 (m, 4H). m/z (ES + APCI)⁺: 436 [M + H]⁺.

trans-N-(3-{4-[(5-Chloro-3-fluoropyridin-2-yl)amino]phenyl}imidazo[1,2-b]pyridazin-6-yl)cyclohexane-1,4-diamine 47. Following the method for **40** using 2,5-dichloro-3-fluoropyridine, we obtained **47** as a yellow solid (13% yield). ¹H NMR (400 MHz, DMSO-*d*₆) δ ppm 9.19 (d, $J = 1.8$ Hz, 1H), 8.18–8.05 (m, 3H), 7.90–7.77 (m, 4H), 7.71 (d, $J = 10.1$ Hz, 1H), 6.91 (d, $J = 6.9$ Hz, 1H), 6.63 (d, $J = 9.6$ Hz, 1H), 3.62–3.43 (m, 1H), 2.72–2.57 (m, 1H), 2.21–2.08 (m, 2H), 1.91–1.76 (m, 3H), 1.33–1.13 (m, 4H). m/z (ES + APCI)⁺: 452 [M + H]⁺.

trans-N-(3-{4-[(3-Fluoro-6-methylpyridin-2-yl)amino]phenyl}imidazo[1,2-b]pyridazin-6-yl)cyclohexane-1,4-diamine 48. Following the method for **40** using 2-bromo-3-fluoro-6-methylpyridine, we obtained **48** as a yellow solid (16% yield). ¹H NMR (400 MHz, DMSO-*d*₆) δ ppm 8.91 (d, $J = 1.8$ Hz, 1H), 8.19–8.03 (m, 2H), 8.03–7.86 (m, 2H), 7.81 (s, 1H), 7.70 (d, $J = 9.6$ Hz, 1H), 7.43 (dd, $J = 7.8$, 11.5 Hz, 1H), 6.91 (d, $J = 6.4$ Hz, 1H), 6.72–6.55 (m, 2H), 3.63–3.46 (m, 1H), 2.70–2.57 (m, 1H), 2.38 (s, 3H), 2.25–2.11 (m, 2H), 1.92–1.81 (m, 2H), 1.39–1.14 (m, 4H). m/z (ES + APCI)⁺: 432 [M + H]⁺.

PfCDPK1 Enzyme Assay. IC₅₀ determinations were performed using Kinase Glo (Promega) to measure ATP depletion resulting from the kinase reaction. Compounds were added to 22 μ L reaction mixtures in white 384-well plates containing 10 nM full length recombinant PfCDPK1 and 8 μ M MyoA-Tail domain Interacting Protein (MTIP) in assay buffer (Tris-HCl buffer at pH 8.0 containing 0.1 mM EGTA, 0.2 mM CaCl₂, 1 mM DTT, and 0.01% Triton X-100) and incubated for 30 min at rt prior to initiating the reaction with 10 μ M ATP (Km) and 20 mM MgCl₂ at final concentrations. Reactions were allowed to proceed for 120 min at ambient temperature and stopped by the addition of 22 μ L of Kinase Glo Plus detection reagent. Luminescence proportional to the remaining ATP at the end of the reaction was measured using a Pherastar plate reader (BMG Labtech). Ten point dose–response curves were obtained from half-log dilutions of the test compound diluted in assay buffer at a constant final DMSO concentration of 1%.

Thermal Denaturation Assay. Purified recombinant PfCDPK1 was diluted to 1 μ M in 10 mM HEPES buffer at pH 7.5 containing 150 mM NaCl, 1 mM Ca²⁺, and 1/1000 SYPRO Orange dye (Invitrogen). Test compounds were prediluted to 400 μ M in 40% v/v DMSO in water, and 1 μ L of diluted compound was added to 39 μ L of enzyme/dye mix in white 96-well quantitative PCR plates (Thermo Scientific) to give a final compound concentration of 10 μ M and preincubated for 30 min at rt. Reference melting temperatures were obtained in parallel by the addition of 1 μ L of 40% v/v DMSO to 39 μ L of diluted PfCDPK1. The plates were sealed with transparent adhesive covers (Biorad) and subjected to a temperature gradient from 25 to 95 K at a rate of 1 K/min using a quantitative PCR machine (MX3005P, Stratagene). Fluorescence data were acquired at 1 min intervals using the FAM/ROX filter set (Ex 492 nm/Em 610 nm) and the raw data exported to Excel (Microsoft) for analysis. Data were processed to

identify the fluorescence maxima and minima, and the midpoints of melting curves were determined by fitting to the Boltzmann equation (XLfit add-in, IDBS software). Results were expressed as ΔT_m values relative to DMSO controls where $\Delta T_m = T_m$ (inhibitor) – T_m (DMSO controls).

P. falciparum in Vitro Parasite Assay. *P. falciparum* EC₅₀ values were measured using an *in vitro* model of malaria parasite growth which measures merozoite invasion of red blood cells. Test cultures were set up at 0.5% parasitemia and 2% hematocrit from a synchronized stock culture of 3D7 *P. falciparum*. Compounds were diluted into 2% DMSO and added to parasites 24 h postinvasion using a 95 μ L parasite culture in a 96-well plate and incubated under static conditions. Compounds were tested at least in duplicate. Cells were recovered 48 h later and processed for FACS analysis: 50 μ L of parasite culture was transferred into a FACS tube and mixed with 500 μ L of 500 μ g/mL hydroethidine in PBS to stain parasite DNA. The parasites were incubated for 20 min at 37 °C, then diluted with 1 mL of PBS, and stored on ice prior to FACS analysis. The data were acquired using CellQuest Pro software on a FACSCalibur (Becton Dickinson). Growth inhibition was calculated using the following formula: % growth inhibition = (1 – [parasitemia of culture/parasitemia of control culture]) \times 100.

PbCDPK1 Enzyme Assay. To establish activity of the compounds against recombinant *P. berghei* CDPK1 enzyme, ATPase activity was measured using a biosensor sensitive to ADP (rhodamine-labeled ParM, gift of M. Webb, NIMR). The progress of the reactions was monitored by an increase in fluorescence corresponding to the accumulation of ADP using a Pherastar plate reader (BMG Labtech).

Kinase Selectivity. Kinase selectivity profiling was carried out at the National Centre for Protein Kinase Profiling in the MRC Protein Phosphorylation Unit at the University of Dundee.

P. berghei Murine in Vivo Efficacy Protocol. *Plasmodium berghei* ANKA strain expressing GFP²⁶ was used. Mice were NMRI females (20–22 g). Compounds were solubilized or suspended in a solution consisting of 70% Tween-80 and 30% ethanol, followed by a 10-fold dilution in H₂O. Chloroquine (Sigma C6628) was used as a control drug. Test procedure: Day 0, from a donor mouse with approximately 30% parasitemia, heparinized blood (containing 50 μ L of 200 u/mL Heparin) is taken and diluted in physiological saline to 10⁸ parasitized erythrocytes per mL. Of this suspension, 0.2 mL was injected intravenously (i.v.) into experimental groups of 3 mice and a control group of 3 mice. Four hours postinfection, the experimental groups were treated with a single dose of compound by the oral (p.o.) route. Days 1–3: 24, 48, and 72 h postinfection, the experimental groups were treated with a single daily dose of compound p.o. at 50 mg/kg. Day 4: 24 h after the last drug treatment, 1 μ L of tail blood was taken and suspended in 1 mL of PBS buffer. Parasitemia was determined with a FACScan (Becton Dickinson) by counting 100'000 red blood cells. The difference of the mean infection rate of the control group (= 100%) to the test group was calculated and expressed as percent reduction. The results are expressed as the reduction of parasitemia on day 4 in % as compared to the untreated control group. As an example, activity determination with a mean of, e.g., 2% parasitemia in treated mice and a mean of, e.g., 40% parasitemia in the control animals is calculated as follows: (40% – 2%)/40% \times 100 = 95% reduction in parasitemia.

P. falciparum Murine in Vivo Efficacy Protocol. Described in ref 24.

In Silico Studies. BLAST was used with the PfCDPK1 sequence (UniProt: P62344) to search the PDB to identify suitable templates for homology modeling. Sequence alignments were generated and structures inspected using the Schrodinger molecular modeling suite, 2010 version.¹⁹ The structure of TgCDPK1 (PDB: 3I7C) was selected as the most suitable template for a variety of reasons including good crystallographic quality and high sequence identity, particularly around the ATP site; of the 49 residues within 6 Å of the crystal ligand, 69% are identical, and 92% are homologous. Homology modeling was carried out using Prime,¹⁹ and further refinements were not required due to the excellent correspondence between the target and template. The resultant structure was prepared for docking studies involving

solvent removal, valence and charge assignment, addition of hydrogen atoms, orientation of ambiguous groups (e.g., amide groups of Asn and Gln), and restrained minimization to relieve residual strain. A docking grid was generated with size and location based on the 3I7C crystal ligand, including optional constraints to prominent H-bonding groups including Tyr148 at the hinge, Glu152 at the entrance to the pocket, and Asp212 of the DFG-loop. Virtual libraries of compounds were enumerated and prepared for docking using LigPrep¹⁹ then docked flexibly using GlideSP¹⁹ with a H-bonding constraint to Tyr148 N-H, outputting up to three diverse poses per ligand. High scoring candidate molecules were prioritized for synthesis following manual inspection and consideration of additional factors such as favorable/unfavorable contacts and ligand strain.

AUTHOR INFORMATION

Corresponding Author

*Phone: +44 0 20 8906 7100. Fax: +44 0 20 8906 7200. E-mail: tim.chapman@tech.mrc.ac.uk.

Notes

The authors declare no competing financial interest.

ACKNOWLEDGMENTS

We thank David Tickle and Sadhia Mahmood at MRCT for *in vitro* ADME, David Whalley for *in vitro* testing against *P. berghei* CDPK1, and Munira Grainger at NIMR for the provision of *P. falciparum* parasites. We are grateful to the Medicines for Malaria Venture for providing support for this project, including Paul Willis, Didier Leroy, and Simon Campbell for their input, Sergio Wittlin at the Swiss Tropical and Public Health Institute for conducting *P. berghei* *in vivo* efficacy studies, Sue Charman and Karen White at the Centre for Drug Candidate Optimisation at Monash University for PK studies, and GlaxoSmithKline Tres Cantos for running the *P. falciparum* SCID mouse model. A.A.H. is funded by the MRC (U117532067) and the EU FP7 Grant agreement 242095 (EviMalar).

ABBREVIATIONS USED

Pf, *Plasmodium falciparum*; *Pb*, *Plasmodium berghei*; CDPK, calcium-dependent protein kinase; MLM, mouse liver microsomes; HLM, human liver microsomes; (A-Phos)₂PdCl₂, bis(di-*tert*-butyl(4-dimethylaminophenyl)phosphine)dichloropalladium(II); CyPF-^tBu, (dicyclohexylphosphino)ferrocenyl]ethyl-di-*tert*-butylphosphine; DIPEA, *N,N*-diisopropylethylamine; Pd₂(dba)₃, tris(dibenzylideneacetone)dipalladium(0); Pd(dppf)Cl₂, 1,1'-bis(diphenylphosphino)ferrocenedichloropalladium(II); SCX, strong cation exchange; Xantphos, 4,5-bis(diphenylphosphino)-9,9-dimethylxanthene; 9-BBN, 9-borabicyclo[3.3.1] nonane

REFERENCES

- (1) World Malaria Report, 2010; World Health Organization. www.who.int/malaria/publications/atoz/9789241564106/en/index.html.
- (2) Petersen, I.; Eastman, R.; Lanzer, M. Drug-resistant malaria: molecular mechanisms and implications for public health. *FEBS Lett.* **2011**, 1551–1562.
- (3) Harper, J. F.; Harmon, A. Plants, symbiosis and parasites: a calcium signalling connection. *Nat. Rev. Mol. Cell. Biol.* **2005**, 6, 555–566.
- (4) Ward, P.; Equinet, L.; Packer, J.; Doerig, C. Protein kinases of the human malaria parasite *Plasmodium falciparum*: the kinome of a divergent eukaryote. *BMC Genomics* **2004**, 5, 79.
- (5) Zhao, Y.; Kappes, B.; Franklin, R. M. Gene structure and expression of an unusual protein kinase from *Plasmodium falciparum*

homologous at its carboxyl terminus with the EF hand calcium-binding proteins. *J. Biol. Chem.* **1993**, 268, 4347–4354.

- (6) Tewari, R.; Straschil, U.; Bateman, A.; Böhme, U.; Cherevach, I.; Gong, P.; Pain, A.; Billker, O. The systematic functional analysis of *Plasmodium* protein kinases identifies essential regulators of mosquito transmission. *Cell Host Microbe* **2010**, 8, 377–387.

- (7) Kato, N.; Sakata, T.; Breton, G.; Le Roch, K. G.; Nagle, A.; Andersen, C.; Bursulaya, B.; Henson, K.; Johnson, J.; Kumar, K. A.; Marr, F.; Mason, D.; McNamara, C.; Plouffe, D.; Ramachandran, V.; Spooner, M.; Tuntland, T.; Zhou, Y.; Peters, E. C.; Chatterjee, A.; Schultz, P. G.; Ward, G. E.; Gray, N.; Harper, J.; Winzeler, E. A. Gene expression and small-molecule compounds link a protein kinase to *Plasmodium falciparum* motility. *Nat. Chem. Biol.* **2008**, 4, 347–356.

- (8) Green, J. L.; Rees-Channer, R. R.; Howell, S. A.; Martin, S. R.; Knuepfer, E.; Taylor, H. M.; Grainger, M.; Holder, A. A. The motor complex of *Plasmodium falciparum*: phosphorylation by a calcium-dependent protein kinase. *J. Biol. Chem.* **2008**, 283, 30980–30989.

- (9) Holder, A. A.; Mohd Ridzuan, M. A.; Green, J. L. Calcium dependent protein kinase 1 and calcium fluxes in the malaria parasite. *Microbes Infect.* **2012**, 14, 825–830.

- (10) Sebastian, S.; Brochet, M.; Collins, M. O.; Schwach, F.; Jones, M. L.; Goulding, D.; Rayner, J. C.; Choudhary, J. S.; Billker, O. A *Plasmodium* calcium-dependent protein kinase controls zygote development and transmission by translationally activating repressed mRNAs. *Cell Host Microbe* **2012**, 12, 9–19.

- (11) Azevedo, M. F.; Sanders, P. R.; Krejany, E.; Nie, C. Q.; Fu, P.; Bach, L. A.; Wunderlich, G.; Crabb, B. S.; Gilson, P. R. Inhibition of *Plasmodium falciparum* CDPK1 by conditional expression of its J-domain demonstrates a key role in schizont development. *Biochem. J.* **2013**, 452, 433–441.

- (12) Kugelstadt, D.; Derrer, B.; Kappes, B. Calcium-Dependent Protein Kinases as Drug Targets. In *Drug Discovery in Infectious Diseases: Apicomplexan Parasites*; Becker, K., Ed.; Wiley-VCH: Weinheim, Germany, 2011; Vol. 2, pp 319–334.

- (13) Lemercier, G.; Fernandez-Montalvan, A.; Shaw, J. P.; Kugelstadt, D.; Bomke, J.; Domostoj, M.; Schwarz, M. K.; Scheer, A.; Kappes, B.; Leroy, D. Identification and characterization of novel small molecules as potent inhibitors of the plasmodial calcium-dependent protein kinase 1. *Biochemistry* **2009**, 48, 6379–6389.

- (14) Lourido, S.; Zhang, C.; Lopez, M. S.; Tang, K.; Barks, J.; Wang, Q.; Wildman, S. A.; Shokat, K. M.; Sibley, L. D. Optimizing small molecule inhibitors of calcium-dependent protein kinase 1 to prevent infection by *Toxoplasma gondii*. *J. Med. Chem.* **2013**, 56, 3068–3077.

- (15) Johnson, S. M.; Murphy, R. C.; Geiger, J. A.; DeRocher, A. E.; Zhang, Z.; Ojo, K. K.; Larson, E. T.; Perera, B. G. K.; Dale, E. J.; He, P.; Reid, M. C.; Fox, A. M. W.; Mueller, N. R.; Merritt, E. A.; Fan, E.; Parsons, M.; Van Voorhis, W. C.; Maly, D. J. Development of *Toxoplasma gondii* calcium-dependent protein kinase 1 (TgCDPK1) inhibitors with potent anti-toxoplasma activity. *J. Med. Chem.* **2012**, 55, 2416–2426.

- (16) Zhang, Z.; Ojo, K. K.; Johnson, S. M.; Larson, E. T.; He, P.; Geiger, J. A.; Castellanos-Gonzalez, A.; White, A. C.; Parsons, M.; Merritt, E. A.; Maly, D. J.; Verlinde, C. L. M. J.; Van Voorhis, W. C.; Fan, E. Benzoylbenzimidazole-based selective inhibitors targeting *Cryptosporidium parvum* and *Toxoplasma gondii* calcium-dependent protein kinase-1. *Bioorg. Med. Chem. Lett.* **2012**, 22, 5264–5267.

- (17) Chapman, T. M.; Osborne, S. A.; Boulloc, N.; Large, J. M.; Wallace, C.; Birchall, K.; Ansell, K. H.; Jones, H. M.; Taylor, D.; Clough, B.; Green, J. L.; Holder, A. A. Substituted imidazopyridazines are potent and selective inhibitors of *Plasmodium falciparum* calcium-dependent protein kinase 1 (PfCDPK1). *Bioorg. Med. Chem. Lett.* **2013**, 23, 3064–3069.

- (18) Ojo, K. K.; Larson, E. T.; Keyloun, K. R.; Castaneda, L. J.; DeRocher, A. E.; Inampudi, K. K.; Kim, J. E.; Arakaki, T. L.; Murphy, R. C.; Zhang, L.; Napuli, A. J.; Maly, D. J.; Verlinde, C. L.; Buckner, F. S.; Parsons, M.; Hol, W. G.; Merritt, E. A.; Van Voorhis, W. C. *Toxoplasma gondii* calcium-dependent protein kinase 1 is a target for selective kinase inhibitors. *Nat. Struct. Mol. Biol.* **2010**, 17, 602–607.

(19) Schrödinger Release 2010, Schrödinger LLC: New York, NY, 2010.

(20) Niesen, F. H.; Berglund, H.; Vedadi, M. The use of differential scanning fluorimetry to detect ligand interactions that promote protein stability. *Nat. Protoc.* **2007**, *2*, 2212–2221.

(21) Peters, W.; Robinson, B. L. Malaria. In *Handbook of Animal Models of Infection*; Zak, O., Sande, M. A., Eds.; Academic Press: San Diego, CA, 1999; pp 757–773.

(22) pK_a values were calculated using *ACD/PhysChem Suite 7*, version 12.01; Advanced Chemistry Development, Inc.: Toronto, ON, Canada. www.acdlabs.com.

(23) Large, J. M.; Osborne, S. A.; Smiljanic-Hurley, E.; Ansell, K. H.; Jones, H. M.; Taylor, D. L.; Clough, B.; Green, J. L.; Holder, A. A. Imidazopyridazines as potent inhibitors of *Plasmodium falciparum* calcium-dependent protein kinase 1 (PfCDPK1): Preparation and evaluation of pyrazole linked analogues. *Bioorg. Med. Chem. Lett.* **2013**, *23*, 6019–6024.

(24) Angulo-Barturen, I.; Jiménez-Díaz, M. B.; Mulet, T.; Rullas, J.; Herreros, E.; Ferrer, S.; Jiménez, E.; Mendoza, A.; Regadera, J.; Rosenthal, P. J.; Bathurst, I.; Pompliano, D. L.; Gómez de las Heras, F.; Gargallo-Viola, D. A murine model of falciparum-malaria by in vivo selection of competent strains in non-myelodepleted mice engrafted with human erythrocytes. *PLoS One* **2008**, *3*, e2252.

(25) Jebiwott, S.; Govindaswamy, K.; Mbugua, A.; Bhanot, P. *Plasmodium berghei* calcium dependent protein kinase 1 is not required for host cell invasion. *PLoS One* **2013**, *8*, e79171.

(26) Franke-Fayard, B.; Trueman, H.; Ramesar, J.; Mendoza, J.; van der Keur, M.; van der Linden, R.; Sinden, R. E.; Waters, A. P.; Janse, C. J. A *Plasmodium berghei* reference line that constitutively expresses GFP at a high level throughout the complete life cycle. *Mol. Biochem. Parasitol.* **2004**, *137*, 23–33.